© 2021. Published by The Company of Biologists Ltd | Journal of Cell Science (2021) 134, jcs252411. doi:10.1242/jcs.252411

RESEARCH ARTICLE

Rab5 regulates macropinocytosis by recruiting the inositol 5-phosphatases OCRL and Inpp5b that hydrolyse PtdIns(4,5)P_2

Michelle E. Maxson[1], Helen Sarantis[1], Allen Volchuk[1], John H. Brumell[1,2,3,4] and Sergio Grinstein[1,5,6,*]

ABSTRACT

Rab5 is required for macropinosome formation, but its site and mode of action remain unknown. We report that Rab5 acts at the plasma membrane, downstream of ruffling, to promote macropinosome sealing and scission. Dominant-negative Rab5, which obliterates macropinocytosis, had no effect on the development of membrane ruffles. However, Rab5-containing vesicles were recruited to circular membrane ruffles, and soluble N-ethylmaleimide-sensitive factor attachment protein receptor (SNARE)-dependent endomembrane fusion was necessary for the completion of macropinocytosis. This fusion event coincided with the disappearance of PtdIns(4,5)P_2 that accompanies macropinosome closure. Counteracting the depletion of PtdIns(4,5)P_2 by expression of phosphatidylinositol-4-phosphate 5-kinase impaired macropinosome formation. Importantly, we found that the removal of PtdIns(4,5)P_2 is dependent on Rab5, through the Rab5-mediated recruitment of the inositol 5-phosphatases OCRL and Inpp5b, via APPL1. Knockdown of OCRL and Inpp5b, or APPL1, prevented macropinosome closure without affecting ruffling. We therefore propose that Rab5 is essential for the clearance of PtdIns(4,5)P_2 needed to complete the scission of macropinosomes or to prevent their back-fusion with the plasmalemma.

KEY WORDS: Macropinocytosis, GTPase, Rab, Phosphatase, Phosphoinositide, EGF, Ruffling

INTRODUCTION

Macropinocytosis is an actin-driven process that involves the formation and extension of plasma membrane ruffles and the eventual closure of large (≥0.2 to 5.0 µm) endocytic vacuoles (Swanson, 2008). Dendritic cells and macrophages perform macropinocytosis constitutively in order to sample their environment for immune surveillance (Bohdanowicz et al., 2013). However, most cell types require stimulation by growth promoters to initiate macropinocytosis (Haigler et al., 1979; Mellström et al., 1988; Racoosin and Swanson, 1989). In these cases macropinocytosis can play an important role in the delivery of extracellular nutrients, including proteins and amino acids, to lysosomes (Bloomfield and Kay, 2016; Racoosin and Swanson, 1992). The significance of macropinocytosis to cellular physiology is illustrated by its common dysregulation in a variety of diseased states; the manipulation of macropinocytosis is a hallmark of cancer metabolism (O'Donnell et al., 2018) and provides an entry gateway for a variety of viruses, including vaccinia and Ebola (Mercer and Helenius, 2012).

The formation of macropinosomes depends on the integration of receptor signalling, phosphoinositide metabolism, activation of small GTPases and the remodelling of the actin cytoskeleton (Buckley and King, 2017; Levin et al., 2014; Marques et al., 2017). Growth factors, such as macrophage colony stimulating factor (M-CSF, also known as CSF1) and epithelial growth factor (EGF), bind to cognate tyrosine kinase receptors and activate signalling cascades that culminate in the recruitment and activation of phosphatidylinositol 3-kinase (PI3K) (Abella et al., 2010; Araki et al., 1996; Cheng et al., 2015; Wang et al., 2001). The resulting generation of phosphatidylinositol-3,4,5-trisphosphate [PtdIns(3,4,5)P_3] is critical for macropinocytosis in a variety of cell types (King and Kay, 2019; Veltman et al., 2016; Welliver and Swanson, 2012). Together with its precursor, phosphatidylinositol-4,5-bisphosphate [PtdIns(4,5)P_2], PtdIns(3,4,5)P_3 promotes the recruitment and activation of small GTPases of the Ras and Rho families that induce the formation of the circular ruffles that precede macropinocytosis (Bar-Sagi and Feramisco, 1986; Fujii et al., 2013; Kay et al., 2018; Porat-Shliom et al., 2008; Welliver et al., 2011). Rho-family GTPases support the recruitment of Arp2/3 and formins that mediate the actin polymerization observed in macropinocytic cups (Junemann et al., 2016; Veltman et al., 2016).

Completion of macropinosome formation requires membrane fusion and is followed by maturation of the resulting vacuole, which proceeds to merge with endosomes and, ultimately, lysosomes. Fusion and maturation are accompanied by rapid disassembly of the rich actin meshwork that initiated ruffling and macropinosome formation. The disassembly is due, at least in part, to the breakdown of PtdIns(3,4,5)P_3 and PtdIns(4,5)P_2 that accompanies macropinosome closure (Araki et al., 2007; Hasegawa et al., 2011; Maekawa et al., 2014; Welliver and Swanson, 2012; Yoshida et al., 2009). Closure is also coincident with the acquisition of small GTPases of the Rab family, notably Rab5 (Araki et al., 2006; Feliciano et al., 2011; Porat-Shliom et al., 2008; Roberts et al., 2000; Welliver and Swanson, 2012). Rab5, a prototypical component of early endosomes, is thought to drive the initial stages of macropinosome maturation. However, expression of dominant-negative Rab5 was found to block macropinocytosis (Feliciano et al., 2011; Roberts et al., 2000), suggesting an additional early role for Rab5 in macropinosome formation. Accordingly, active Rab5 has been localized to the plasma membrane during macropinocytosis (Bucci et al., 1992; Chavrier et al., 1990; Lanzetti et al., 2004). However, at this time, the manner whereby Rab5 affects macropinosome formation remains unclear. We therefore revisited the role of Rab5 in macropinocytosis.

[1]Program in Cell Biology, Hospital for Sick Children, Toronto, Ontario M5G 0A4, Canada. [2]SickKids IBD Centre, Hospital for Sick Children, Toronto, Ontario M5G 0A4, Canada. [3]Institute of Medical Science, University of Toronto, Toronto, Ontario M5S 1A1, Canada. [4]Department of Molecular Genetics, University of Toronto, Toronto, Ontario M5S 1A1, Canada. [5]Department of Biochemistry, University of Toronto, Toronto, Ontario M5S 1A8, Canada. [6]Keenan Research Centre for Biomedical Science, St. Michael's Hospital, Toronto, Ontario M5B 1W8, Canada.

*Author for correspondence (sergio.grinstein@sickkids.ca)

H.S., 0000-0001-9416-3975; S.G., 0000-0002-0795-4160

Handling Editor: Daniel Billadeau
Received 29 July 2020; Accepted 25 February 2021

Journal of Cell Science (2021) 134, jcs252411. doi:10.1242/jcs.252411

RESULTS

Rab5 is necessary for the completion of macropinocytosis

Serum-starved A431 cells respond quickly to the addition of EGF with plasmalemmal ruffling and the formation of 1.5-2 µm-sized macropinosomes (Fabricant et al., 1977; Haigler et al., 1979). We chose this well-established model system to investigate the role of Rab5 in macropinocytosis. As expected, in the absence of EGF, A431 cells internalized little tetramethylrhodamine-conjugated 70 kDa dextran (TMR-D), a prototypical marker of macropinocytic uptake, and uptake was unchanged by expression of wild-type Rab5A (Fig. 1A, left panel). After incubation with EGF, Rab5A^{+} cells internalized TMR-D robustly (Fig. 1A, right panel), as did non-transfected neighbouring cells (not shown). In contrast, EGF-treated A431 cells expressing a dominant-negative version of Rab5A (Rab5A$_{S34N}$) failed to internalize TMR-D, whereas the non-transfected neighbouring cells did (Fig. 1B). Expression of Rab5A$_{S34N}$ decreased macropinocytosis by 86.8% (Fig. 1C, black bars), in agreement with earlier findings (Feliciano et al., 2011; Roberts et al., 2000). Because expression of dominant-negative alleles can have pleiotropic effects, e.g. by inhibiting exchange factors shared by multiple GTPases, we validated the requirement for Rab5 by silencing the three Rab5 isoforms; the combined use of siRNA to the A, B and C isoforms decreased the overall expression of Rab5 by 88.1±4.3% (n=4), as assessed by immunoblotting (not shown). This collective silencing depressed TMR-D uptake by 73% (Fig. 1C, grey bars), validating the specific involvement of Rab5 in macropinosome formation.

Macropinocytosis entails the development of membrane ruffles and their closure to form sealed vacuoles. We therefore sought to define whether Rab5 is required for the extension of ruffles or, instead, for their sealing. To this end, the dynamics of macropinosome formation was monitored by time-lapse video microscopy, using the N-terminal domain of Lyn (Lyn$_{11}$) tagged with RFP to selectively visualize the plasma membrane. This region of Lyn is myristoylated and palmitoylated, effectively targeting the Lyn$_{11}$-RFP construct to the plasma membrane and nascent macropinosomes. Temporal projections of A431 cells expressing Lyn$_{11}$-RFP revealed the extensive ruffling elicited by treatment with

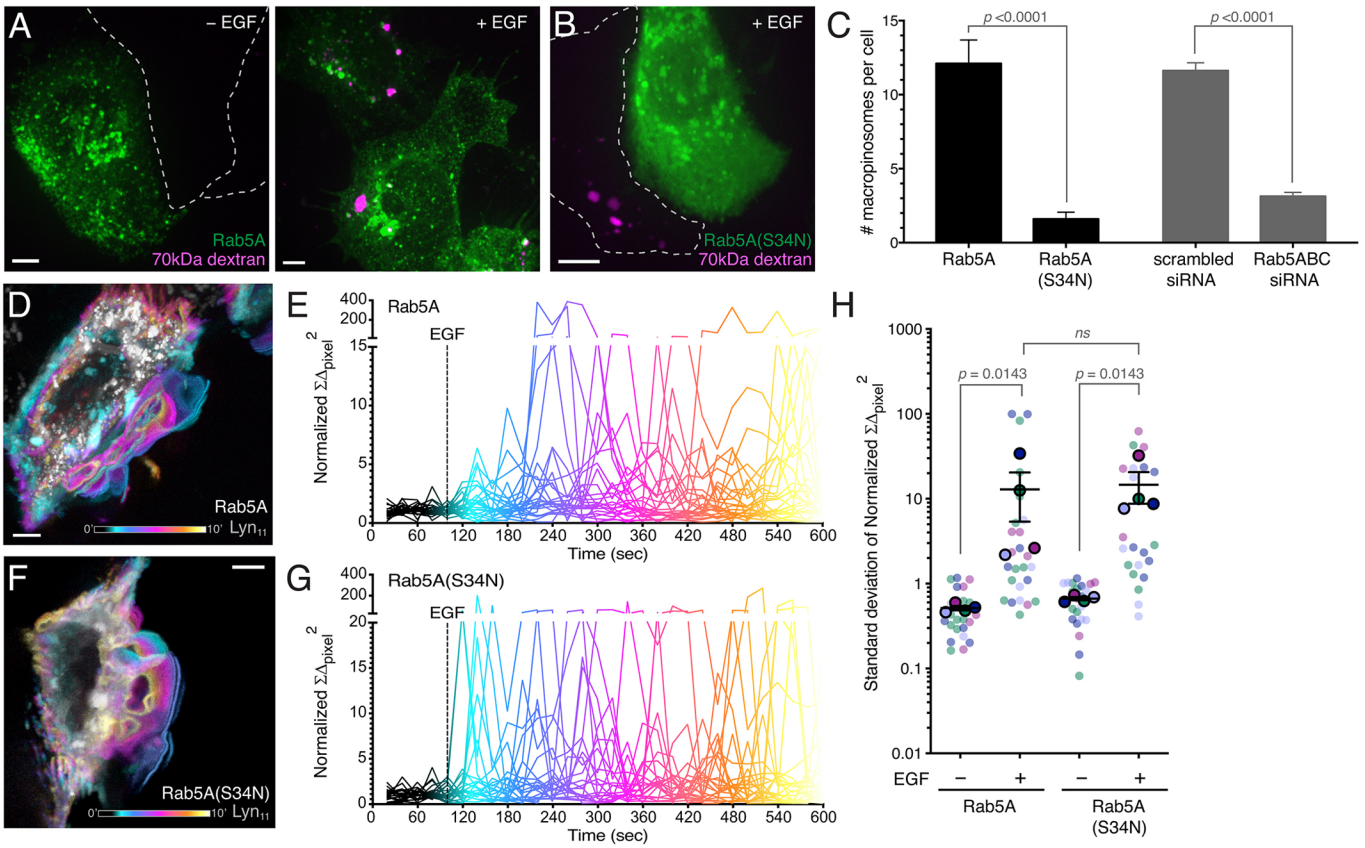

Fig. 1. Rab5 is required for the completion of macropinocytosis but not for cell ruffling. Macropinocytosis was induced in A431 cells by EGF (see Materials and Methods). (A) Effect of Rab5A overexpression. Extended focus visualization of TMR-D uptake by GFP-Rab5A-expressing cells in the absence (left) or presence (right) of EGF. TMR-D is shown in magenta. The outlines of untransfected A431 cells are indicated by dashed lines. (B) Effect of Rab5A$_{S34N}$ overexpression. Extended focus visualization of TMR-D uptake by GFP-Rab5A$_{S34N}$-expressing cells stimulated by EGF. (C) After EGF treatment in the presence of TMR-D, transiently transfected or siRNA-treated A431 monolayers were visualized and the number of macropinosomes per cell counted by confocal microscopy. For each condition, ≥5 independent experiments were quantified, with ≥10 cells per replicate. Data are mean±s.e.m. (D) Temporal projection of cellular ruffling Rab5A-expressing cells over a 10 min incubation with EGF. GFP-Rab5A is pseudocoloured white, Lyn$_{11}$-RFP is pseudo-coloured as a function of time using the 'cool' LUT. A colour-coded temporal scale is included. (E) Quantification of ruffling for Rab5A-expressing cells over a 10 min timespan. Individual cells are represented by separate traces. N=23. Lines are temporally pseudocoloured as in D. The addition of EGF is indicated by dotted vertical line. A detailed description of normalized $\Sigma\Delta^2_{pixel}$ calculation can be found in Materials and Methods. (F) Temporal projection of cellular ruffling Rab5A$_{S34N}$-expressing cell stimulated with EGF as in D. Images in A-F are representative of ≥30 fields from ≥3 separate experiments of each type. (G) Quantification of ruffling for Rab5A$_{S34N}$-expressing cells, as in E, N=22. (H) Scatter plot of s.d. of the normalized $\Sigma\Delta^2_{pixel}$ values in the experiments illustrated in E and F. Rimmed circles indicate means of individual experiments, identified by colour-coding. Data are mean±s.e.m. of four replicates. Statistical significance was determined using an unpaired two-tailed Student's t-test (C) or a Mann–Whitney test (H). ns, not significant. Scale bars: 5 µm.

Journal of Cell Science (2021) 134, jcs252411. doi:10.1242/jcs.252411

EGF (e.g. Fig. 1D). Importantly ruffling was qualitatively indistinguishable in cells that were co-transfected with Lyn_{11}-RFP and either wild-type Rab5A or $Rab5A_{S34N}$ (Fig. 1D,F; Movies 1, 2). A more rigorous comparison of the effects of the wild-type and dominant-negative forms of Rab5 was made by measuring the sum of the differences in fluorescence intensity ($\Sigma\Delta_{pixel}$) associated with membrane displacement (i.e. ruffling). The differences were squared ($\Sigma\Delta^2_{pixel}$) to eliminate the cancelling effects of positive versus negative changes in fluorescence intensity. As shown in Fig. 1E,G, where the behaviour of multiple individual cells is compared, membrane positioning changed comparatively little over time before the addition of EGF, but marked oscillations were apparent upon addition of the growth factor. Comparison of the s.d. of the $\Sigma\Delta^2_{pixel}$ in the period before and after the addition of EGF confirmed that the ruffling triggered by the growth factor was similar in cells expressing Rab5A or $Rab5A_{S34N}$ (Fig. 1H). We therefore concluded that functional Rab5 is not required for membrane ruffling and that the GTPase is instead involved in another downstream step in vacuole generation.

Rab5 is recruited to plasmalemmal circular ruffles before macropinosome closure

Because Rab5 is seemingly not required for ruffling, we considered the possibility that it is instead involved in macropinosome sealing. This would require the engagement of the GTPase before closure of the macropinocytic vacuole. Rab5 has been reported to be present in macropinosome membranes shortly after closure (Feliciano et al., 2011; Roberts et al., 2000), but the precise timing of its acquisition has not been established. It is possible that Rab5 is involved in the sealing of the macropinosome; alternatively, Rab5 may play a role in stabilizing the nascent macropinosome, preventing its back-fusion with the plasma membrane. In accordance with the earlier reports, we routinely observed Rab5 merging with nascent macropinosomes within ∼4 min of EGF addition (Fig. 2A). While examining the macropinocytic process by time-lapse microscopy we observed the striking recruitment and tight apposition of GFP-$Rab5A^+$ endocytic vesicles to emerging circular ruffles/early macropinosomes as early as ∼1 min after EGF addition (Fig. 2A,B; Movie 3).

When acquiring optical slices by confocal microscopy it is not possible to conclusively differentiate between open circular ruffles and sealed vacuoles. This strategy alone was therefore insufficient to establish whether the tight apposition and fusion of Rab5 vesicles occur before macropinosome sealing. To more definitively establish the timing of Rab5 recruitment, we induced macropinocytosis with EGF for 2 min in the presence of TMR-D, then rapidly chilled the cells to arrest the process and stained them with the membrane-impermeant dye FM4-64. FM4-64, which is brightly fluorescent only when intercalated into membranes, was viewed immediately (< 5 min) to prevent its endocytic uptake. Thus, only the plasma membrane, which is continuously exposed to the extracellular milieu, as well as open (but not sealed) macropinosomes, was expected to show dye fluorescence. Conversely, only macropinosomes were expected to retain TMR-D. Strikingly, we found that $Rab5A^+$ vesicles were distinctly recruited to circular ruffles that had not closed, identified as round structures that were nearly continuous yet stained clearly with FM4-64; multiple examples are illustrated in transverse (*X* versus *Y*; bottom) and in orthogonal reconstructions (*X* versus *Z*; top) in Fig. 2C. These structures did not retain TMR-D (Fig. 2C, left), which was instead retained by $FM4\text{-}64^-$ macropinosomes (Fig. 2C, right). To ensure that these observations were not an artifactual result of Rab5A overexpression, we also examined the distribution of the early endocytic compartment in EGF-treated cells by immunostaining endogenous EEA1, a Rab5 ligand and effector (Simonsen et al., 1998). As described for ectopically expressed Rab5A, $EEA1^+$ vesicles localized to membrane ruffles and open circular ruffles (visualized using plasmalemmal PLCδ-PH as a marker) before macropinosome closure (Fig. 2D). Although we cannot ascertain that the recruited endosomes had fused with open circular ruffles, these data indicate that tight apposition of $Rab5^+$ organelles precedes macropinosome closure.

Rab5 plays a role at the plasma membrane promoting the completion of macropinocytosis

Because Rab5-containing vesicles were recruited to circular ruffles at early stages of macropinosome formation (Fig. 2), and genetic inhibition of Rab5 blocked macropinocytosis (Fig. 1B,C), we investigated whether their attachment and/or fusion with the plasma membrane is required to promote macropinosome formation. To this end, we expressed plasma membrane targeted chimeras of wild-type Rab5A, $Rab5A_{Q67L}$ – a constitutively active variant – and the dominant-negative $Rab5A_{S34N}$ fused to the 20 C-terminal amino acids of K-Ras4B. This sequence includes a CAAX motif and a polylysine sequence that jointly target the chimeric construct to the plasma membrane (Galperin and Sorkin, 2003). Expression of these constructs did not have a noticeable effect on endocytosis, as measured by internalization of transferrin (Fig. 3A,B, insets). Interestingly, expression of wild-type or constitutively active Rab5A at the plasma membrane was neither sufficient to induce macropinocytosis – measured as TMR-D internalization – in the absence of EGF (Fig. 3A), nor did it prevent macropinocytosis induced by EGF (Fig. 3B). In contrast, plasmalemmal $Rab5A_{S34N}$-CAAX robustly inhibited macropinocytosis (Fig. 3B,C), in a manner indistinguishable from that observed for $Rab5A_{S34N}$ expressed in the cytosol, which partitions into the membrane by virtue of its geranylgeranylation (Fig. S1B; Fig. 3B,C).

Additionally, we recapitulated these results using an inducible rapamycin heterodimerization system (iRAP) to recruit CFP-FKBP-Rab5A or $Rab5A_{S34N}$ to the plasma membrane (using Lyn_{11}-FKB). Rapamycin-induced recruitment of CFP-FKBP-Rab5A was not sufficient to induce macropinocytosis in the absence of EGF, but recruitment of CFP-FKBP-$Rab5A_{S34N}$ blocked macropinocytosis in EGF-stimulated cells (Fig. S1), consistent with the results obtained with CAAX-tagged versions of the GTPase. Jointly, these observations suggest that the dominant-negative effect of $Rab5A_{S34N}$ on macropinocytosis is exerted at the plasma membrane.

Endogenous inactive GDP-bound Rab5 is thought to reside in the cytosol, complexed with Rab GDI, and the active GTP-bound form associates with early endocytic membranes (Zerial and McBride, 2001). During macropinocytosis, it was conceivable that Rab5 could be activated/recruited to the plasma membrane from the cytosol, or be acquired through fusion of endocytic vesicles containing active Rab5, as suggested by the observations in Fig. 2. To distinguish between these mechanisms, we adapted a reverse dimerization system (Rivera et al., 2000) to acutely block soluble N-ethylmaleimide-sensitive factor attachment protein receptor (SNARE)-mediated membrane fusion with dominant-negative N-ethylmaleimide-sensitive factor (NSF_{E329Q}). Expression of this reverse dimerization construct (EGFP-F_M4-NSF_{E329Q}) results in the formation of multimeric aggregates in the cytosol, due to the presence of four tandem mutant FKBP (F_M4) domains in the construct, which can be solubilized promptly by the addition of a cell-permeant rapamycin analog (Fig. 3D). Due to the acute release of NSF_{E329Q}, the cells do not experience the toxicity normally seen when expressing soluble dominant-negative NSF for extended periods (Coppolino et al., 2001).

Journal of Cell Science (2021) 134, jcs252411. doi:10.1242/jcs.252411

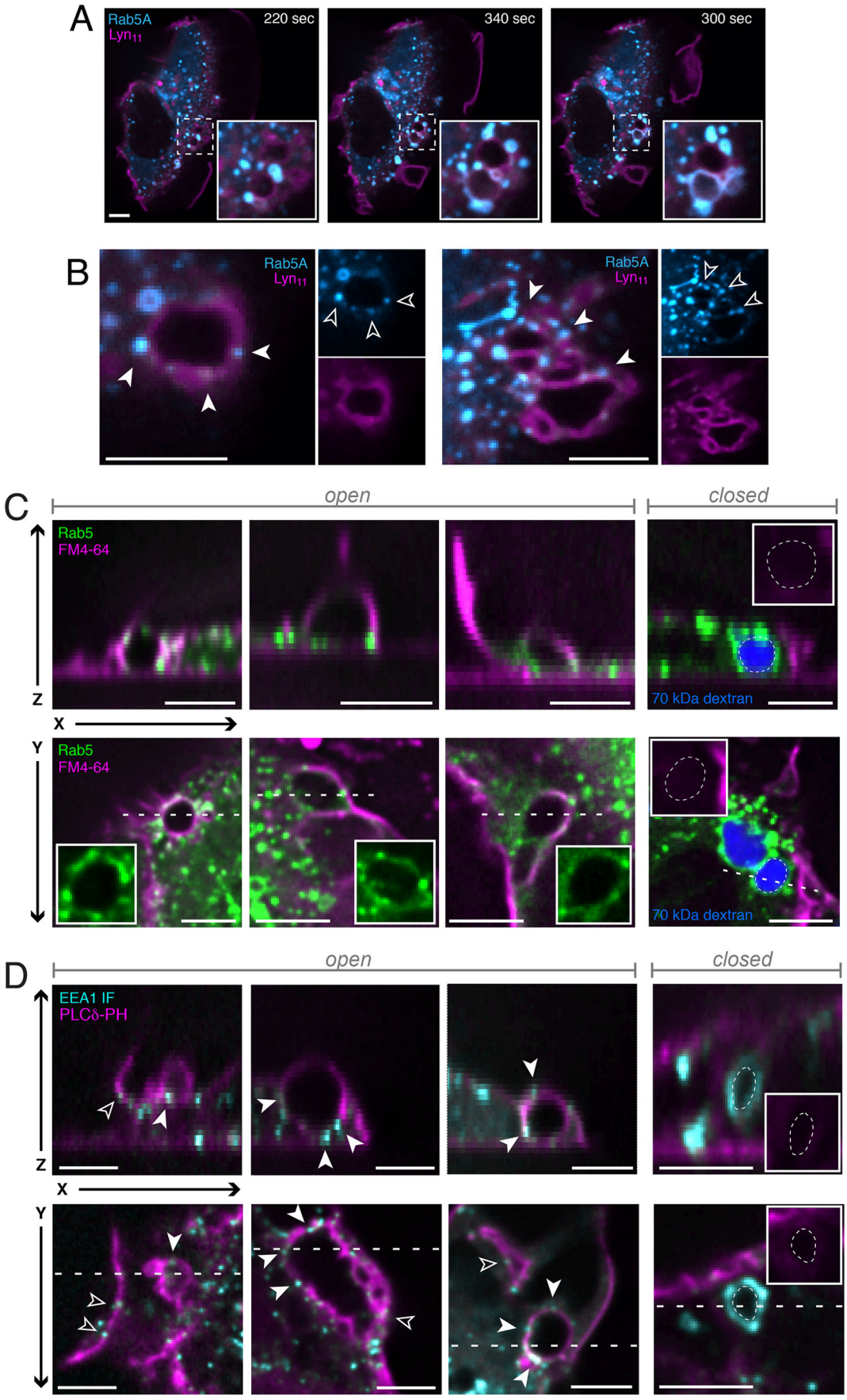

Fig. 2. See next page for legend.

Journal of Cell Science (2021) 134, jcs252411. doi:10.1242/jcs.252411

Fig. 2. Rab5A is recruited to circular ruffles and open macropinocytic cups. (A) Rab5A localization to nascent macropinosomes. Confocal visualization of cells expressing GFP-Rab5A (cyan) and Lyn_{11}-RFP (magenta), treated with EGF to induce macropinocytosis. The time after stimulation when images were acquired is indicated. Insets are 2.8× magnifications of the area in the dashed square. (B) Localization of GFP-Rab5A (cyan) in plasma membrane ruffles visualized with Lyn_{11}-RFP (magenta) during EGF-induced macropinocytosis. Arrowheads mark $Rab5^+$ vesicles apposed to ruffles. Insets show individual Rab5A and Lyn_{11} channels. (C) Macropinocytosis was induced by EGF in A431 cells expressing GFP-Rab5A, and after 2 min, cells were cooled and visualized by confocal microscopy. Surface membranes and open macropinosomes were visualized by FM4-64 staining (see Materials and Methods). The localization of Rab5A (green) and FM4-64 (magenta) in *XZ* reconstructions (top) and individual *XY* optical slices (bottom) are shown for three representative open macropinosomes and one closed macropinosome, as indicated. Closed macropinosomes retained TMR-D, shown in blue. The dashed line across the *XY* slice represents the location of the corresponding *XZ* reconstruction. Insets are 1.6, 1.1, 1.2 and 1.3× magnification (left to right). (D) Macropinocytosis was induced in A431 cells expressing RFP-PLCδ-PH by treatment with EGF for 10 min. Surface membranes and open macropinosomes were delineated by PLCδ-PH (magenta) and endogenous early endocytic compartment was detected by immunostaining EEA1 (cyan; see Materials and Methods). The localization of EEA1 and PLCδ-PH in *XZ* reconstructions (top) and individual *XY* optical slices (bottom) are shown for three representative open macropinosomes and one closed macropinosome, as indicated. Arrowheads mark $EEA1^+$ vesicles apposed to ruffles (open arrowheads) or circular ruffles (closed arrowheads). The dashed line across the *XY* slice represents the location of the corresponding *XZ* reconstruction. Scale bars: 5 µm.

As expected, when expressed in A431 cells, EGFP-F_M4-NSF_{E329Q} formed large cytosolic aggregates (Fig. 3E, left) that were functionally inconsequential. This was verified by monitoring the appearance of the Golgi complex, which was unaffected by the aggregated form of the dominant-negative NSF (Fig. S2A). As expected, aggregated EGFP-F_M4-NSF_{E329Q} also did not affect macropinocytosis (Fig. 3E,F). The EGFP-F_M4-NSF_{E329Q} aggregates dissociated gradually upon addition of the D/D solubilizer (Fig. S3E). The appearance of soluble EGFP-F_M4-NSF_{E329Q} was accompanied by inhibition of endomembrane fusion, as evinced by the fragmentation and dispersal of the Golgi complex (Fig. S2A, right). Importantly, solubilization of the dominant-negative NSF caused a profound (92%) inhibition of macropinocytosis (Fig. 3E,F). Of note, the membrane ruffling induced by EGF was unaffected by the soluble NSF_{E329Q} (Fig. S2B) and $Rab5^+$ endosomes, seemingly coated with NSF_{E329Q}, were found in the vicinity of actin-rich circular ruffles (Fig. 3G). We therefore concluded that a SNARE-mediated fusion event, possibly that of Rab5-containing vesicles with the plasma membrane, is required for macropinocytosis. However, an indirect effect of NSF_{E329Q} cannot be ruled out.

Rab5 contributes to the depletion of PtdIns(4,5)P_2 at the macropinocytic cup, which is required for macropinosome sealing

Loss of PtdIns(4,5)P_2, which is abundant in the plasma membrane, is one of the early events that accompany macropinosome formation (Porat-Shliom et al., 2008; Welliver and Swanson, 2012). While examining EGF-induced macropinocytosis by time-lapse microscopy, we observed that the docking of $Rab5A^+$ endocytic vesicles onto circular ruffles preceded the loss of PtdIns(4,5)P_2 (Fig. 4A). Strikingly, expression of dominant-negative $Rab5A_{S34N}$ prolonged the presence of PtdIns(4,5)P_2 on circular ruffles (Fig. 4B), suggesting that active Rab5 is normally required for the depletion of the inositide. These observations suggested that PtdIns(4,5)P_2 depletion may be required for the completion of macropinocytosis.

This notion was tested by expressing the genetically encoded PtdIns(4,5)P_2 biosensor PLCδ-PH-GFP in cells also expressing Lyn_{11}-RFP, used to visualize the membrane and nascent macropinosomes. As expected, PtdIns(4,5)P_2 was present in the plasma membrane and was clearly visible in the ruffles induced by EGF (Fig. 4C; Movie 4). As reported previously (Porat-Shliom et al., 2008; Welliver and Swanson, 2012), PtdIns(4,5)P_2 was lost from the macropinosome membrane as it internalized (Fig. 4C, right; Movie 4). The loss of PtdIns(4,5)P_2 from the macropinosome membrane was associated with the retention of TMR-D, the hallmark of closed macropinosomes (Fig. 4D). This inverse correlation was analysed in detail by measuring the abundance of PLCδ-PH-GFP on Lyn_{11}-RFP^+ cups/vesicles over time and comparing it to the retention of TMR-D. Numerous circular ruffles containing high PtdIns(4,5)P_2 and little TMR-D were observed 5 min after stimulation with EGF (Fig. 4E). Between 10 and 20 min the number of vacuoles retaining TMR-D increased progressively as the PtdIns(4,5)P_2 levels decreased (Fig. 4E; Fig. S3A). Analysis of these populations (Fig. S3B) showed the vesicles fell into well-defined groups: those that were open (i.e. devoid of TMR-D) and contained PtdIns(4,5)P_2, and those that were seemingly closed (i.e. able to retain TMR-D) and depleted of PtdIns(4,5)P_2. There were virtually no sealed vesicles that retained PtdIns(4,5)P_2. Taken together, these data confirmed that PtdIns(4,5)P_2 localized predominantly to open macropinocytic cups, and was depleted quickly at the time of macropinosome sealing or shortly thereafter.

These observations raised the possibility that PtdIns(4,5)P_2 depletion is in fact required for the completion of macropinocytosis or to prevent macropinosome back-fusion with the plasmalemma. To examine this possibility, we sought to prevent this depletion by overexpressing the type I PtdIns 4-phosphate 5-kinase (PIP5K), which catalyzes the conversion of plasmalemmal PtdIns(4)P to PtdIns(4,5)P_2. When expressed heterologously in A431 cells, the GFP-tagged α and β isoforms of PIP5K localized to the plasma membrane, in which they effectively blocked macropinocytic retention of TMR-D by 76.2% and 76.3%, respectively, compared to cells expressing GFP only (Fig. 4F,G). Notably, expression of a kinase-dead version of PIP5Kβ, which is normally targeted to the membrane, did not block macropinocytosis, indicating that the catalytic activity of PIP5K, and thus the overproduction of PtdIns(4,5)P_2, is responsible for blocking the completion of macropinocytosis. Temporal projections of A431 cells expressing Lyn_{11}-RFP to visualize the plasma membrane confirmed that the plasma membrane underwent ruffling upon EGF addition in cells expressing PIP5Kβ-GFP or $PIP5K\beta_{KD}$-GFP; this ruffling was indistinguishable from that of EGF-stimulated cells co-expressing GFP (Fig. S4), suggesting that expression of the kinases did not interfere grossly with actin dynamics. Instead, we interpreted these data to mean that the sustained presence of PtdIns(4,5)P_2 in the circular ruffle blocks macropinosome sealing.

Rab5 effectors Inpp5b, OCRL and APPL1 localize to macropinocytic cups and vesicles, and are required for macropinosome sealing

The timing of Rab5 acquisition and loss of PtdIns(4,5)P_2 from forming phagosomes led us to question whether the two events are causally related. The mammalian 5-phosphatases Inpp5b and OCRL, which can degrade PtdIns(4,5)P_2, are both Rab5-associating effectors implicated in endocytosis and macropinocytosis (Fukuda et al., 2008; Hyvola et al., 2006; Loovers et al., 2007; Mao et al., 2009; Shin et al., 2005; Swan et al., 2010; Williams et al., 2007). Therefore, these phosphatases were likely candidates to catalyze the observed

Journal of Cell Science (2021) 134, jcs252411. doi:10.1242/jcs.252411

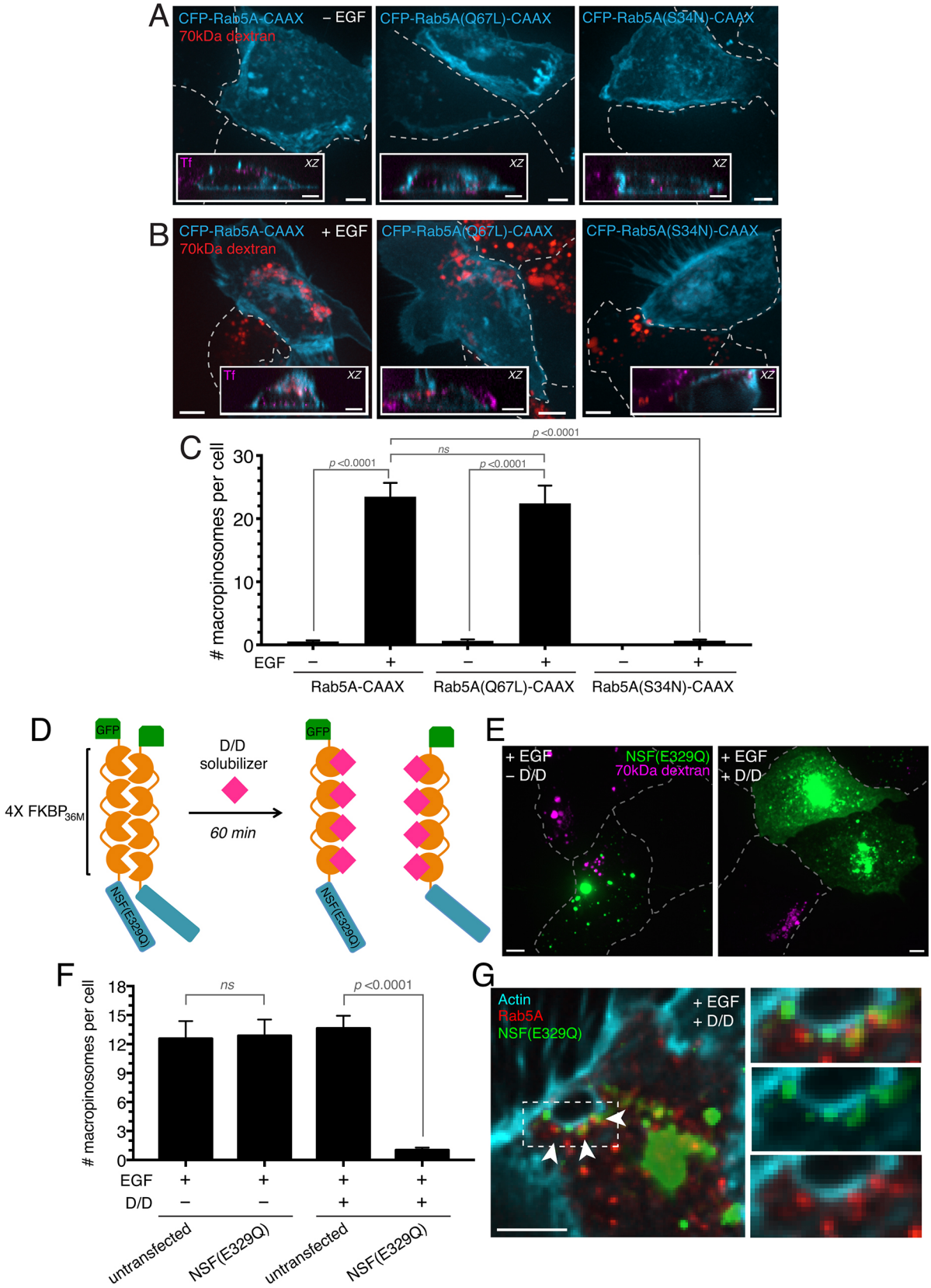

Fig. 3. See next page for legend.

PtdIns(4,5)P_2 depletion. Inpp5b and OCRL can interact with Rab5 directly, or interact with endomembranes by way of another Rab5 effector, APPL1 (Bohdanowicz et al., 2011; Erdmann et al., 2007; Swan et al., 2010; Zhu et al., 2007). We observed that soon after stimulation by EGF, punctate structures containing Inpp5b and OCRL – likely endomembrane vesicles – were recruited to

Journal of Cell Science

Journal of Cell Science (2021) 134, jcs252411. doi:10.1242/jcs.252411

Fig. 3. Rab5A localization to the plasma membrane, through SNARE-mediated fusion events, is necessary for the completion of macropinocytosis. (A) Effect of Rab5-CAAX constructs on the macropinocytosis and endocytosis. Cells transfected with CFP-Rab5A-CAAX, CFP-Rab5A$_{Q67L}$-CAAX or CFP-Rab5A$_{S34N}$-CAAX (cyan) were incubated with TMR-D (red) in the absence of EGF. Early endocytic compartments were visualized following a 5 min loading with transferrin (magenta). Main panels are extended focus images of the cyan and red channels only. A paucity of TMR-D taken up in the absence of EGF can be observed. Inset: orthogonal (*x* versus *z*) image showing internalized transferrin and the plasmalemmal localization of the CAAX-tagged constructs. (B) Effect of Rab5-CAAX constructs on the completion of macropinocytosis. Cells were transfected with CFP-Rab5A-CAAX (cyan), CFP-Rab5A$_{Q67L}$-CAAX or CFP-Rab5A$_{S34N}$-CAAX and incubated with TMR-D (red) in the presence of EGF. Insets as in A. (C) The number of macropinosomes per cell was counted as described in Materials and Methods. For each condition, three independent experiments were quantified, with ≥10 cells per replicate. (D) Schematic representation of the reverse aggregation of the F$_M$4-NSF$_{E329Q}$ construct tagged with EGFP. When expressed in mammalian cells, EGFP-F$_M$4-NSF$_{E329Q}$ aggregates spontaneously but aggregation is reversed upon addition of D/D solubilizer, allowing for acute inhibition of SNARE-mediated vesicle fusion. (E) Cells expressing EGFP-F$_M$4-NSF$_{E329Q}$ (green) were incubated in the absence of (left) or 60 min after the addition of D/D solubilizer (right). Cells were then treated with EGF plus TMR-D, as described in Materials and Methods. Following fixation, transfected cells and untransfected neighbours were monitored for the retention of TMR-D (magenta). (F) Cells treated as in E were fixed, and the number of macropinosomes per cell were counted by confocal microscopy in transfected cells and untransfected neighbours. For each condition, three independent experiments were quantified, with ≥10 cells per replicate. (G) Cells expressing EGFP-F$_M$4-NSF$_{E329Q}$ and Rab5A-RFP were treated as in E and stained with phalloidin (cyan) following fixation. Insets are 1.8× magnifications of the area in the dashed square. Arrowheads mark NSF$_{E329Q}$ and Rab5A double-positive vesicles apposed to ruffles. Images in A, B, E and G are representative of ≥30 fields from ≥3 separate experiments of each type. Data are mean±s.e.m. Statistical significance was determined using an unpaired two-tailed Student's *t*-test. ns, not significant. The outlines of untransfected A431 cells are indicated by dashed lines in A, B and E. Scale bars: 5 µm.

PtdIns(4,5)P$_2^+$ plasma membrane ruffles (Fig. 5A) in a manner similar to that observed for Rab5. Notably, APPL1 was also recruited in this fashion (Fig. 5A, right). Time-lapse imaging revealed that the recruitment of Inpp5b, OCRL and APPL1 preceded the loss of PtdIns(4,5)P$_2$ from macropinocytic cups (Fig. S5A-C). Like the analogous early recruitment of Rab5$^+$ vesicles, we interpreted this as evidence that the docking of Inpp5b-, OCRL- and APPL1-bearing vesicles occurred before macropinosomes sealed (Fig. S5D-F). Extensive acquisition of Inpp5b, OCRL and APPL1 was obvious on macropinosomes that retained TMR-D, and were therefore closed (Fig. 5B), consistent with earlier findings (Swan et al., 2010; Wall et al., 2018; Zoncu et al., 2009). The requirement for APPL1 for the recruitment of the 5-phosphatases was tested using siRNA-mediated silencing. When APPL1 expression was suppressed by 85.9% (Fig. S6A), APPL1-depleted cells recruited considerably less OCRL to Rab5-containing endosomes: the Manders' (M) coefficient was M$_{red}$=0.280, compared to M$_{red}$=0.785 in cells treated with scrambled RNA (Fig. 5C,D). This was consistent with previous findings that APPL1 cooperates with Rab5 to recruit 5-phosphatases to endosomes and phagosomes (Bohdanowicz et al., 2011; Erdmann et al., 2007).

The functional requirement of these Rab5 effectors for macropinocytosis was then assessed by RNA-mediated silencing. The 5-phosphatases were silenced individually or together, and APPL1 was silenced as well. The effectiveness of the silencing protocol was assessed: the expression of Inpp5b was reduced by 80.9% and that of OCRL by 77.8%, when silenced separately (Fig. S6B). When silenced jointly, expression was suppressed by 82.1% and 77.7% for Inpp5b and OCRL, respectively. APPL1 silencing was the most effective, reaching 95.9% (Fig. S6B). The effects of these treatments on macropinocytosis were assessed next. Inhibiting the expression of either Inpp5b or OCRL caused a marked reduction in macropinocytic efficiency, and simultaneous silencing of both phosphatases resulted in an even greater reduction (~85%; Fig. 5E). The extent of the latter was comparable to the one attained by silencing APPL1 (Fig. 5E).

These findings are consistent with the notion that APPL1 cooperates with Rab5 in the recruitment of OCRL and Inpp5b. We therefore used APPL1-silenced cells to further assess the role of PtdIns(4,5)P$_2$ breakdown by the phosphatases in the macropinocytic process. The effect of downregulating the adaptor on membrane ruffling was investigated using the same approaches introduced earlier. Visualization (Fig. 5F versus H; compare also Movie 5 versus Movie 6) and quantitative analysis (Fig. 5G,I,J) of ruffling in cells transfected with Lyn$_{11}$-RFP showed no significant differences between cells treated with scrambled siRNA and those silenced using APPL1-directed siRNA, which responded normally to stimulation by EGF. These findings reinforce the conclusion that depletion of PtdIns(4,5)P$_2$ occurs after plasma membrane ruffling and is likely involved in macropinosome sealing.

Recruitment of yeast Inp54 to the plasma membrane bypasses the dominant-negative effect of Rab5A$_{S34N}$ on macropinocytosis

Jointly, the preceding observations suggest that Rab5 may participate in macropinosome sealing by recruiting Inpp5b and OCRL, which facilitate sealing by dephosphorylation of PtdIns(4,5)P$_2$. If this model were true, we hypothesized that it would be possible to bypass the inhibitory effect of Rab5A$_{S34N}$ by recruiting to the plasma membrane an alternative heterologous 5-phosphatase capable of hydrolysing PtdIns(4,5)P$_2$ while the cells are undergoing EGF-induced ruffling. We chose the yeast 5-phosphatase Inp54 as it is exquisitely specific for PtdIns(4,5)P$_2$ (Raucher et al., 2000; Stolz et al., 1998). As before, we used an iRAP system to recruit Inp54 to the plasma membrane of cells expressing either Rab5A or Rab5A$_{S34N}$. These cells were co-transfected with YFP-FKBP-Inp54 plus the plasma membrane-localizing Lyn$_{11}$-FKB construct. The addition of rapamycin resulted in the rapid recruitment of Inp54 to the plasma membrane (Fig. 6A, insets). As expected, macropinocytosis proceeded normally in cells expressing Rab5A, regardless of whether Inp54 was recruited or not to the membrane (Fig. 6A, top panels). However, although cytosolic Inp54 was not able to overcome the effect of dominant-negative Rab5A on macropinocytosis, the phosphatase enabled TMR-D uptake when recruited to the membrane at the time of EGF stimulation (Fig. 6A, bottom panels). Recruitment of Inp54 to the plasma membrane restored macropinocytosis to levels similar to cells expressing wild-type Rab5A (Fig. 6B). Taken together, these findings confirm that the breakdown of PtdIns(4,5)P$_2$ to PtdIns(4)P in the macropinocytic cup is critical for the completion of macropinocytosis. Active Rab5 plays an essential role in this process by recruiting to the macropinocytic cup 5-phosphatase activity required for sealing, exerted primarily by OCRL and Inpp5b, which are recruited through the adaptor APPL1.

DISCUSSION

The involvement of Rab5 in macropinocytosis has been known for decades, but its mode of action remained enigmatic and controversial. Some reports concluded that Rab5 operated at the plasma membrane, promoting ruffling (Barbieri et al., 1998; Lanzetti et al., 2004; Spaargaren and Bos, 1999), whereas others disputed this claim and proposed instead a role for Rab5 only after

Journal of Cell Science (2021) 134, jcs252411. doi:10.1242/jcs.252411

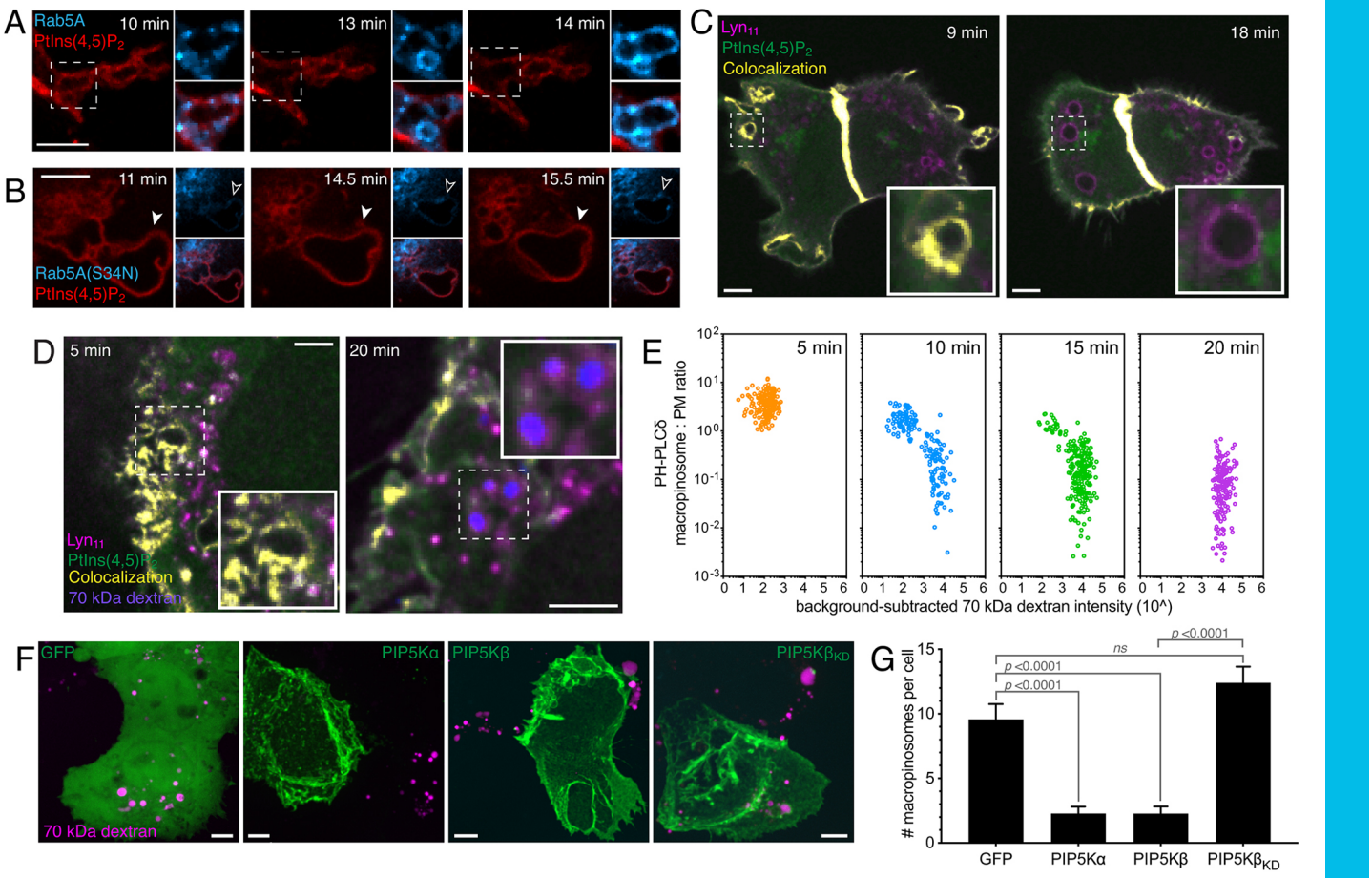

Fig. 4. PtdIns(4,5)P_2 disappearance from forming macropinosomes is necessary for macropinosome closure. (A) Live cell visualization of PtdIns(4,5)P_2 using PLCδ-PH-RFP (red) in cells co-expressing GFP-Rab5A (cyan), at indicated times after EGF addition. Panel insets: Rab5A and merged channels, at 2× magnification. (B) Visualization of PLCδ-PH-RFP (red) in cells co-expressing GFP-Rab5A$_{S34N}$ (cyan), at indicated times after EGF addition. Panel insets: Rab5A$_{S34N}$ and merged channels. Closed arrowheads mark PtdIns(4,5)P_2 ruffles, that do not recruit vesicles (open arrowheads). Panel insets: Rab5A$_{S34N}$ and merged channels, at 1× magnification. (C) Live cell visualization of PtdIns(4,5)P_2 using PLCδ-PH-GFP (green) and the plasma membrane using Lyn$_{11}$-RFP (magenta) in EGF-treated cells, at indicated time points. EGF addition occurred between the 150-180 s time points. Colocalization of PLCδ-PH-GFP with Lyn$_{11}$-RFP shown in yellow. Images in the insets are at 4× magnification. (D) Cells transfected with PLCδ-PH-GFP (green) and Lyn11-RFP (magenta) were treated with EGF in the presence of TMR-D, as described in Materials and Methods. Retention of TMR-D (blue) was visualized by fixing cells 5 min or 20 min after EGF addition, followed by serial confocal imaging and extended focus projection. Colocalization of PLCδ-PH-GFP with Lyn$_{11}$-RFP shown in yellow. Images in the insets are at 1.7× magnification. (E) Plots of PLCδ-PH-GFP macropinosome:plasma membrane ratio versus background-subtracted TMR-D intensity for all Lyn$_{11}$-RFP$^+$ macropinocytic circular ruffles/vacuoles, determined at 5, 10, 15 and 20 min after EGF addition. Number of vacuoles quantified: 5 min, 177; 10 min, 184; 15 min, 225; 20 min, 179. (F) Monolayers transfected with GFP, GFP-PIP5Kα, GFP-PIP5Kβ or GFP-PIP5Kβ$_{KD}$ (all in green) were treated with EGF in the presence of TMR-D, as described in Materials and Methods. Following fixation, retention of TMR-D (magenta) was imaged as above. Images in A-F are representative of ≥30 fields from ≥3 separate experiments of each type. (G) Cells treated as in F were fixed, and the number of macropinosomes per cell were counted by confocal microscopy. For each condition, three independent experiments were quantified, with ≥10 cells per replicate. Data are means±s.e.m. Statistical significance was determined using an unpaired two-tailed Student's *t*-test. ns, not significant. Scale bars: 5 µm.

vacuole internalization (Feliciano et al., 2011; Roberts et al., 2000). Here, we demonstrate that breakdown of PtdIns(4,5)P_2 is a central requirement for the formation and/or persistence of sealed macropinosomes, a mechanism dependent on Rab5 and its effectors APPL1, Inpp5b and OCRL. These effectors may enable sealing and detachment of the nascent vacuole, or may prevent its back-fusion with the plasma membrane, which would negate the internalization event.

Our findings suggest that Rab5 exerts its effects before the scission of the nascent macropinocytic vacuole from the surface membrane. Accordingly, dominant-negative Rab5 prevents formation of the vacuole while not affecting the occurrence of membrane ruffling. The docking and likely fusion of Rab5-decorated vesicles with circular ruffles before sealing is consistent with this conclusion, as is the observation that the dominant-negative form of the GTPase is inhibitory when recruited to the plasmalemma constitutively or through heterodimerization. Using current technology it is impossible to unambiguously ascertain that Rab5$^+$ vesicles in fact fuse with the surface membrane before macropinosome scission, but experiments in which fusion was precluded support this notion. Briefly, we implemented a new system whereby a dominant-negative form of NSF was acutely released into the cytosol of the test cells, obviating the detrimental non-specific effects associated with long-term expression of such inhibitory constructs. Blocking membrane fusion using this comparatively rapid manoeuvre caused a profound inhibition of macropinocytosis. Although the resolution limits of light microscopy do not yet allow for dynamic visualization of vesicle-circular ruffle fusion, these data are highly suggestive of the requirement for focal fusion of endomembranes with the plasma membrane during macropinocytosis, analogous to what has been

Journal of Cell Science (2021) 134, jcs252411. doi:10.1242/jcs.252411

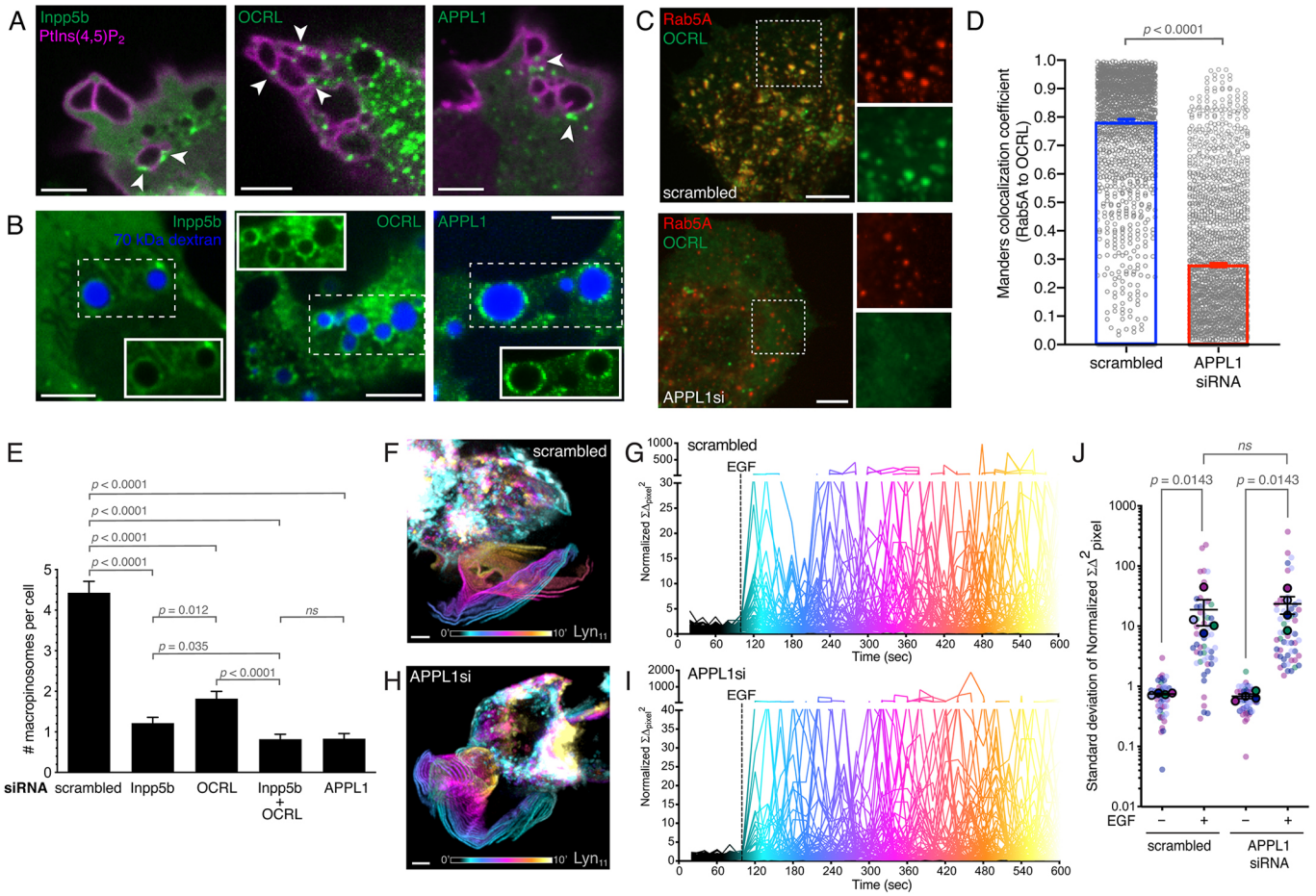

Fig. 5. Role of Inpp5b, OCRL and APPL1 in macropinocytosis. (A) Macropinocytosis was induced by EGF addition in cells expressing GFP-tagged Inpp5b, OCRL or APPL1 (green), with PLCδ-PH-RFP (magenta). Arrowheads indicate apposition of Inpp5b$^+$, OCRL$^+$ or APPL1$^+$ vesicles onto PtdIns(4,5)P_2^+ macropinocytic ruffles/vacuoles. (B) Monolayers transfected with GFP-tagged Inpp5b, OCRL or APPL1 (green) were treated with EGF in the presence of TMR-D, as described in Materials and Methods. Following fixation, retention of TMR-D was imaged (blue). Insets show GFP-tagged Inpp5b, OCRL or APPL1 channels alone. (C) Effect of siRNA-mediated silencing of APPL1 on the colocalization of Rab5 (red) and OCRL (green). Monolayers were treated with indicated siRNAs for 48 h, and transfected with Rab5-RFP and OCRL-GFP. (D) Scatter bar plot displaying mean (bar) and individual values (points) for a Manders' colocalization analysis of Rab5A-RFP with OCRL-GFP in scrambled- (blue) or APPL1si-treated (red) cells. Data are mean±s.e.m. of three replicates. Scrambled, *N*=1529; APPL1si, *N*=1835. (E) Effect of siRNA-mediated gene silencing of Inpp5b, OCRL, Inpp5b plus OCRL, or APPL1 on macropinocytosis. Monolayers were treated with indicated siRNAs for 48 h, then treated with EGF in the presence of TMR-D. Macropinosome formation was scored as described in Materials and Methods. For each condition, three independent experiments were quantified, with ≥10 cells per replicate. Data are mean±s.e.m. (F) Temporal projection of cellular ruffling in Lyn_{11}-RFP-expressing cells treated with control (scrambled) siRNA. Cells were stimulated with EGF and ruffling visualized over 10 min. See Fig. 1D for details. (G) Quantification of ruffling in cells treated with control (scrambled) siRNA. *N*=48. Addition of EGF indicated by dashed vertical line. See Fig. 1E for details. (H) Temporal projection of cellular ruffling in Lyn_{11}-RFP-expressing cells treated with APPL1 siRNA. Cells were stimulated with EGF and ruffling was visualized over 10 min. Images are representative of ≥30 fields from ≥3 separate experiments of each type. (I) Quantification of ruffling in cells treated with APPL1 siRNA. *N*=53. (J) Scatter plot of s.d. of the normalized $\Sigma\Delta^2_{pixel}$ values in the experiments illustrated in G and I. Rimmed circles indicate the means of individual experiments, identified by colour-coding. Data are mean±s.e.m. of four replicates. Statistical significance was determined using an unpaired two-tailed Student's *t*-test (D,E) or a Mann–Whitney test (J). ns, not significant. Scale bars: 5 µm.

reported for phagocytosis (Bajno et al., 2000; Braun et al., 2004). The sealing of macropinosomes is accompanied by loss of PtdIns(4,5)P_2 from their limiting membrane (Porat-Shliom et al., 2008; Welliver and Swanson, 2012), an observation we were able to verify (Fig. 4). Although firmly documented in the past, the functional implications of the disappearance of the inositide were unclear. Our data suggest a correlation between PtdIns(4,5)P_2 depletion and macropinosome sealing, although temporal and resolution limits of live-cell imaging warrant caution when assigning causation. Most pertinently, hydrolysis of the inositide on circular ruffles failed to occur when Rab5 activity was impaired (Fig. 4B), suggesting that Rab5 functions upstream of this event. Moreover, preventing the depletion of PtdIns(4,5)P_2 by enhancing its rate of synthesis, through overexpression of PIP5K, precluded macropinosome formation. These findings led us to postulate that PtdIns(4,5)P_2 hydrolysis from forming macropinosomes is essential for their scission from the membrane and/or to prevent their back-fusion with the surface membrane. Rapid PtdIns(4,5)P_2 hydrolysis accompanies endosome and phagosome formation also, and may be a common feature and requirement of all endocytic pathways.

We noted that docking of Rab5 to circular ruffles preceded PtdIns(4,5)P_2 depletion from the macropinocytic cup (Fig. 4A) and therefore postulated a role for the GTPase in the hydrolysis of the phosphoinositide. Our subsequent experiments provided a plausible mechanism: we propose that through the adaptor APPL1, Rab5 recruits Inpp5b and OCRL to the membrane, two active

Journal of Cell Science (2021) 134, jcs252411. doi:10.1242/jcs.252411

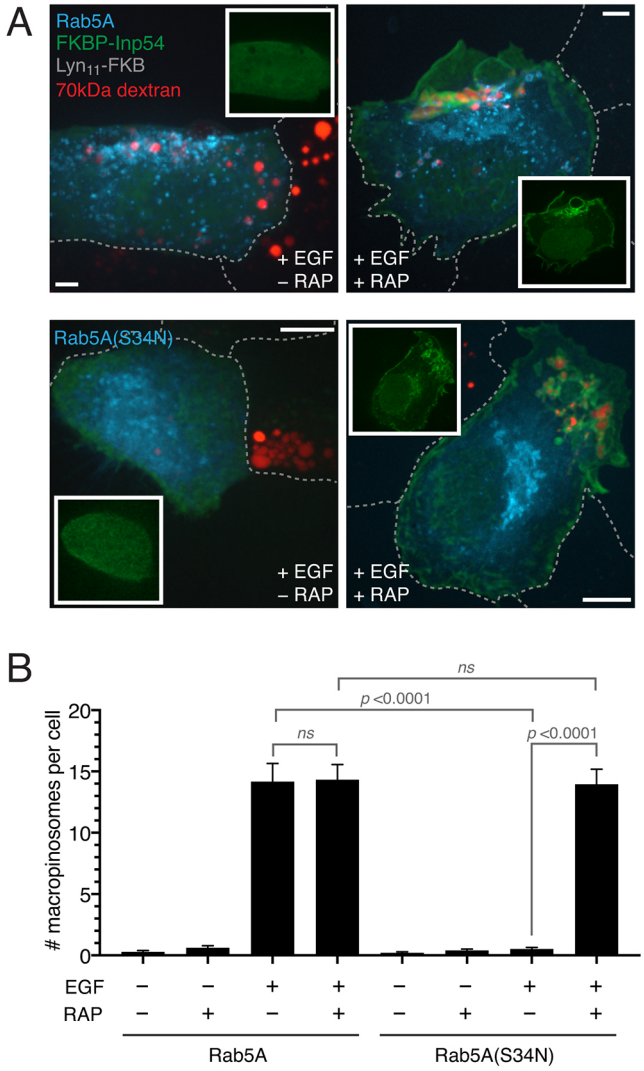

Fig. 6. Depletion of PtdIns(4,5)P_2 by recruitment of a 5-phosphatase overcomes the inhibitory effect of dominant-negative Rab5A on macropinosome closure. (A) Plasma membrane recruitment of Inp54 in Rab5A- or Rab5A$_{S34N}$-expressing cells (cyan) was induced by rapamycin-dependent dimerization of FKBP-Inp54 (green) to Lyn$_{11}$-FKB. Monolayers were treated with EGF±rapamycin in the presence of TMR-D, as described in Materials and Methods. Following fixation, retention of TMR-D (red) was visualized in extended focus images. Insets show a single *XY* slice illustrating the localization of Inp54. Images are representative of ≥30 fields from ≥3 separate experiments of each type. The outlines of untransfected A431 cells are indicated by dashed lines. (B) Effect of Inp54 recruitment on the number of macropinosomes formed per cell. Cells treated as in A were fixed, and the number of macropinosomes per cell were counted by confocal microscopy. For each condition, four independent experiments were quantified, with ≥10 cells per replicate. Data are mean±s.e.m. Statistical significance was determined using an unpaired two-tailed Student's *t*-test.
ns, not significant. Scale bars: 5 µm.

phosphatases capable of degrading PtdIns(4,5)P_2 to PtdIns(4)P. The adaptor, as well as the phosphatases, is recruited to nascent macropinosomes (Fig. 5A,B) and, more importantly, their depletion greatly inhibits macropinocytosis without altering membrane ruffling (Fig. 5E,I).

Dephosphorylation by Inpp5b and OCRL is not solely responsible for the elimination of PtdIns(4,5)P_2 from macropinosomes. Welliver and Swanson (2012) and Yoshida et al. (2015) had clearly demonstrated earlier that phospholipase C contributes to the process, generating diacylglycerol and Ins(1,4,5)P_3. We believe that the initial hydrolysis of PtdIns(4,5)P_2 is caused by phospholipase C, whereas the final stages of its removal, which occur at the time of sealing, are catalyzed by Inpp5b and OCRL. Alternatively, phospholipase C activity may predominate at the base of the macropinocytic cup, while the phosphatases may be most active at the singular point at which sealing occurs. According to this scenario, restoration of inositol phosphatase activity should bypass the inhibition of macropinocytosis by dominant-negative Rab5. Indeed, using an inducible heterodimerization system we found that macropinocytosis could be restored in cells expressing Rab5A$_{S34N}$ by recruiting an exogenous phosphatase, Inp54, to the membrane at the time of stimulation with EGF (Fig. 6A,B).

In summary, our experiments have defined the mechanism by which Rab5 and its associated inositol 5-phosphatases OCRL and Inpp5b catalyze macropinosome sealing. The hydrolysis of PtdIns(4,5)P_2 occurs in the macropinocytic cup as a result of the recruitment and eventual fusion of early endosomes containing Rab5 and its effectors. These data serve to highlight the intricate intersection between cytoskeletal dynamics, small GTPase activity and phosphoinositide signalling that occurs during dynamic cellular uptake processes, such as macropinocytosis.

MATERIALS AND METHODS

Reagents

Mammalian expression vectors were obtained from the following sources: GFP-Rab5A (Roberts et al., 2000); GFP-Rab5A$_{S34N}$ (35141, Addgene); CFP-Rab5A (Heo et al., 2006); CFP-Rab5A$_{S34N}$ (Heo et al., 2006); RFP-Rab5A (Chen et al., 2009); mCherry-Rab5A$_{S34N}$ (35139, Addgene); PLCδ-PH-GFP (Stauffer et al., 1998); PLCδ-PH-RFP (Stauffer et al., 1998); Lyn$_{11}$-RFP (Lee et al., 2007); GFP-PIP5Kα (Fairn et al., 2009); GFP-PIP5Kβ (Fairn et al., 2009); GFP-PIP5Kβ$_{KD}$ (Fairn et al., 2009); pC$_4$S$_1$-EGFP-F$_M$4-FCS-hGH (Ariad Pharmaceuticals; Rivera et al., 2000); NSF$_{E329Q}$ (Coppolino et al., 2002); GFP-APPL1 (Zoncu et al., 2009); Inpp5b-GFP (Williams et al., 2007); OCRL-GFP (Swan et al., 2010); Lyn$_{11}$-FKB (20147, Addgene); CFP-FKBP (20160, Addgene) YF-FKBP-Inp54 (Suh et al., 2006); CFP-Rab5A-CAAX (Galperin and Sorkin, 2003); CFP-Rab5A$_{Q67L}$-CAAX (Galperin and Sorkin, 2003); and CFP-Rab5A$_{S34N}$-CAAX (Galperin and Sorkin, 2003).

Primary antibodies were purchased from the following vendors: Rab5 (3547, Cell Signaling Technology), α-tubulin (T5168, Sigma-Aldrich), GM130 (610822, BD Pharmingen), EEA1 (sc-6451; Santa Cruz Biotechnology). Horseradish peroxidase (HRP), Alexa-568- and Alexa-647-conjugated secondary antibodies against mouse IgG were from Jackson ImmunoResearch Labs.

Cell culture

The A431 cell line was obtained from and authenticated by the American Type Culture Collection (ATCC). Before experimentation, this cell line was revalidated by assessing the expression of epithelial membrane markers (E-cadherin and β-catenin), and responsiveness to EGF. A431 cells were grown in Dulbecco's modified Eagle Medium (DMEM) containing (MultiCell, Wisent) and 10% heat-inactivated fetal calf serum, at 37°C under 5% CO_2. The cell line tested negative for mycoplasma contamination by DAPI staining.

Macropinocytosis assays

A431 cells were plated on 18 mm glass coverslips at a concentration of 1.5×10^5 cells ml^{-1} in DMEM containing L-glutamine and 10% heat-inactivated FCS at 37°C and 5% CO_2. The next day, the medium was changed to Hank's balanced salt solution (HBSS) (311-515-CL; MultiCell, Wisent), and cells were serum starved for 3 h at 37°C. Cells were treated for 20 min with 200 ng ml^{-1} EGF (Invitrogen, Thermo Fisher Scientific), in the presence of 100 µg ml^{-1} TMR-D (Molecular Probes, Thermo Fisher Scientific). Monolayers were rinsed three times with PBS, placed in

HBSS and imaged live. The cells were visualized at the indicated intervals after the addition of EGF±TMR-D (5, 10, 15, 20 min).

To distinguish sealed macropinosomes from open circular ruffles, A431 cells were serum starved for 3 h at 37°C and incubated for 2 min with 200 ng ml^{-1} EGF and 100 µg ml^{-1} TMR-D. Cells were then washed three times with cold 1× PBS, and stained for 1 min with 20 µM FM4-64 (Invitrogen, Thermo Fisher Scientific) at 10°C. Samples were viewed immediately by confocal microscopy. In some cases, after EGF treatment, monolayers were fixed in 3% paraformaldehyde for 10 min at room temperature. Monolayers were blocked/permeabilized in PBS containing 5% BSA and 0.1% saponin, and stained with antibody to EEA1 (1:100 dilution in blocking buffer), followed by fluorescently conjugated secondary antibody (1:1000 dilution in blocking buffer).

DNA transfection

For transient transfection, A431 cells were plated on 18 mm glass coverslips at 1.5×10^5 cells ml^{-1}, 16-24 h before the experiments. Lipofectamine LTX with PLUS reagent (Invitrogen, Thermo Fisher Scientific) was used according to the manufacturer's instructions. A431 cells were transfected at a 3:1 ratio using 1.5 µl Lipofectamine LTX, 0.5 µg DNA and 0.5 µl of PLUS reagent per well for 4 h in Opti-MEM medium (Gibco, Thermo Fisher Scientific). Following this, medium was changed to DMEM containing L-glutamine and 10% heat-inactivated FCS, and cells were used for experiments 16 h after transfection.

siRNA gene silencing

siRNAs for Rab5 isoforms A, B and C were obtained from Sigma-Aldrich, based on previously described sequences (Huang et al., 2004). ON-TARGETplus human siRNA SMARTpools targeting APPL1 (L-005138-00-0005), Inpp5b (L-021811-00-0005) and OCRL (L-01-0026-00-005) were obtained from Dharmacon, along with an ON-TARGETplus non-targeting pool (D-001810-10-20). siRNA delivery was performed using either Nucleofector Kit V (Lonza) or a Neon transfection system (Life Technologies, Thermo Fisher Scientific), according to the manufacturers' protocols. For nucleofection of Rab5a/b/c siRNA, 1×10^6 A431 cells were resuspended in 100 µl of Nucleofector Solution T, containing 200 pmol of Rab5a/b/c siRNA, and electroporated with program X-01 on the Nucleofector I system (Lonza). Cells were used 48 h after siRNA treatment. For Neon transfection of APPL1/Inpp5b/OCRL siRNA smart-pools, A431 cells were resuspended to 5×10^6 cells ml^{-1}, and 100 µl of suspension mixed with 200 pmol siRNA. Electroporation was then performed using two 20 ms pulses of 1400 V. After electroporation, cells were immediately transferred to DMEM containing L-glutamine and 10% heat-inactivated FCS, before seeding on coverslips at a concentration of 1.25×10^5 cells ml^{-1}. siRNA-treated cells were used for macropinocytosis experiments 48 h after electroporation. In some cases, after 24 h, cells were transiently transfected with mammalian expression vectors as described above.

siRNA-mediated knockdown was confirmed at 48 h by either western blotting or qPCR. For Rab5A/B/C knockdown, cells were lysed in Laemmli buffer (Bio-Rad). Lysates were separated by SDS-PAGE, followed by transfer to a polyvinylidene difluoride membrane. The membrane was blocked in TBS containing 5% bovine serum albumin (BSA) and 0.05% Tween 20 for 30 min at room temperature, followed by primary antibody staining for 1 h at room temperature in blocking buffer. Primary antibody dilutions were as follows: Rab5 (1:1000); and α-tubulin (1:1000, loading control). After washing the membrane in TBS containing 0.05% Tween 20, samples were incubated 30 min at room temperature with an HRP-conjugated secondary antibody at a 1:5000 dilution. Blots were visualized using the ECL Prime Western Blot detection reagent (GE Healthcare) on film.

For validation of APPL1, Inpp5b and OCRL knockdown, RNA was isolated from siRNA-treated cells using the GeneJET RNA Purification kit (Thermo Fisher Scientific). An aliquot of 1 µg of RNA was used for single strand cDNA synthesis with the SuperScript VILO cDNA Synthesis kit (Invitrogen, Thermo Fisher Scientific). Quantitative PCR was performed using the TaqMan System (Applied Biosystems, Thermo Fisher Scientific) and TaqMan Fast Advanced Mastermix (Applied Biosystems, Thermo Fisher Scientific) on a Step One Plus Real-Time PCR thermal cycler (Step One software v2.2.2; Applied Biosystems, Thermo Fisher Scientific). The Taqman gene expression assays for the reference gene (GAPDH – ID# Hs02786624_g1) and target genes (APPL1 – ID# Hs00179382_m1; Inpp5b – ID# Hs00299982_m1; OCRL – ID# Hs00240844_m1) were duplexed in triplicate. Target gene expression was determined by quantification relative to the GAPDH reference gene and the non-targeting pool control sample ($\Delta\Delta C_T$ method; Livak and Schmittgen, 2001).

Rapamycin-inducible system for targeted protein translocation

For Rab5 iRAP, full length human Rab5A or Rab5A(S34N) were excised from GFP expression vectors using HindIII/BamHI or XhoI/BamHI sites, respectively. These fragments were cloned downstream of CFP-FKBP using the same sites, and co-expressed in cells with the Lyn_{11}-FRB plasma membrane localizing sequence. Treatment of A431 cells with 2.5 µM rapamycin mediated the rapid translocation of FKBP-CFP-Rab5A/Rab5A(S34N) to the plasma membrane by induced heterologous dimerization of rapamycin-binding FKBP and FKB domains. After 5 min pre-treatment with rapamycin, macropinocytosis assays (TMR-D uptake) were performed as described above in the presence of rapamycin. iRAP experiments using YFP-FKBP-Inp54 and Lyn_{11}-FRB, to recruit Inp54 to the plasma membrane upon addition of rapamycin, were performed similarly.

In vitro reverse dimerization system

pC_4S_1-EGFP-F_M4-FCS-hGH is a part of an *in vitro* reverse dimerization system (Ariad Pharmaceuticals; Rivera et al., 2000). This vector contains a CMV enhancer/promoter (C), the secretion signal sequence of human growth hormone (S), EGFP, four tandem repeats of rapalogue-binding $FKBP_{36M}$ (F_M4), and the human growth hormone coding sequence (hGH) downstream of a furin cleavage signal (FCS). To create a reverse dimerization construct for NSF_{E329Q}, the pC_4S_1-EGFP-F_M4-FCS-hGH vector was modified by cloning. The hGH signal sequence was removed using EcoRI/XbaI digestion, and replaced with a synthetic Kozak sequence. Next, the FCS-hGH SpeI/BamHI fragment was replaced with NSF_{E329Q}. The resultant vector, pC_4-EGFP-F_M4-NSF_{E329Q}, generates a protein that undergoes spontaneous aggregation that reverses upon the addition of D/D solubilizer (635054; Takara Bio), a cell-permeant rapamycin analog that binds to the F_M4 domains (see Fig. 3E).

A431 cells were transiently transfected with pC_4-EGFP-F_M4-NSF_{E329Q}, as described above. Transfected monolayers were then serum-starved in HBSS for 2 h, the last hour of which included treatment with 500 nM D/D solubilizer or vehicle (DMSO) control. Macropinocytosis assays were performed as above. The reverse dimerization of NSF_{E329Q} was confirmed in transfected monolayers by assessment of the effect of pC_4-EGFP-F_M4-NSF_{E329Q} expression±D/D solubilizer on Golgi morphology, using immunostaining. Briefly, 1 h after treatment with 500 nM D/D solubilizer or vehicle (DMSO) control, transfected monolayers were fixed in 3% paraformaldehyde for 10 min at room temperature. Monolayers were blocked/permeabilized in PBS containing 5% BSA and 0.1% saponin, and stained with antibody to GM130 (1:500 dilution in blocking buffer), followed by fluorescently conjugated secondary antibody (1:1000 dilution in blocking buffer).

Confocal microscopy and image analysis

Confocal images were acquired using a Yokogawa CSU10 spinning disk system (Quorum Technologies). Images were acquired using a 63×/1.4 NA oil objective or a 25×/0.8 NA water objective (Zeiss), as indicated, with an additional 1.5× magnifying lens. For live experiments, cells were maintained at 37°C using an environmental chamber (Live Cell Instruments). Routine analyses were performed using Volocity software (Perkin Elmer) or Fiji (Schindelin et al., 2012).

For some colocalization analyses, Volocity software was used to calculate positive product of the differences of the mean channels (Li et al., 2004), which were then overlaid on merged images for visualization. Alternatively, Manders' overlap coefficients were calculated in Volocity for individual $Rab5A^+$ endosomes.

For fluorescence intensity calculations, background-subtracted intensities per unit area for expressed fluorescent protein constructs or endogenous proteins (immunofluorescence) were measured in Volocity software. Ratios were calculated comparing relative intensities of transfected markers in the macropinosome membrane compared to plasma membrane, as indicated in

the text. All statistics were calculated using GraphPad Prism software (GraphPad Software).

For the quantification of ruffling, a Java plug-in (Ruffle_Analysis.java; www.doi.org/10.6084/m9.figshare.12349967) was written for Fiji to analyse background-subtracted ruffling movies of EGF-treated A431 cells expressing Lyn_{11}-RFP. Movies were recorded for 2 min pre-EGF and 8 min post-EGF treatment (200 ng ml^{-1}). For a selected region of the ruffling plasma membrane, the plug-in calculates a summed squared pixel difference within a user defined region of interest (ROI), between $frame_{n+1}$ and $frame_n$, for every frame pair in a background-subtracted time-lapse (background subtracted $\Sigma\Delta^2_{pixel}$). The code first takes each individual pixel value within a square/rectangular ROI and subtracts it from the corresponding pixel value in the next frame (Δ_{pixel}). Next, the differences are squared (Δ^2_{pixel}) to eliminate the cancelling effects of positive versus negative changes in fluorescence intensity. Finally, these values are then summed generating a ($\Sigma\Delta^2_{pixel}$) value for each frame, starting with $frame_{n+1}$. For normalization, background-subtracted $\Sigma\Delta^2_{pixel}$ values were normalized to the mean pre-EGF values. For each cell, the s.d. of the background-subtracted $\Sigma\Delta^2_{pixel}$ for the pre-EGF period was compared to that of the post-EGF period, as a metric of the continuous intensity changes/pixel that are seen in an ROI during plasma membrane ruffling. Additionally, temporal projections of A431 cells pre- and post-EGF treatment were generated in Fiji using the included Temporal Color Code plug-in (Daste et al., 2017) and cool LUT. Data calculations and normalizations were performed using Microsoft Excel software. All statistics were calculated using GraphPad Prism software.

General methodology and statistics

Experiments were, for the most part, *in vitro* imaging determinations of individual cells. As such, samples were assigned to groups according to specific experimental treatments (control versus experimental group) applied by the observer/investigator. The number of individual experiments and the number of determinations per experiment were selected to attain an estimate of the variance compatible with the statistical tests used, primarily Student's *t*-test. Each type of experiment was performed a minimum of three separate times (biological replicates) and a minimum of ten individual event determinations (equivalent but not identical to technical replicates). Data were tested for normality, and appropriate testing was applied. No data were excluded as outliers.

Acknowledgements

We thank Dr Philip Ostrowski for writing the ruffle quantification Fiji plug-in, and Dr Michal Bohdanowicz for the construction of the Rab5A and $Rab5A_{S34N}$ iRAP constructs. The plasmid for the reverse dimerization system was kindly provided by Dr Victor Rivera (Ariad Pharmaceuticals, Cambridge, MA, USA).

Competing interests

The authors declare no competing or financial interests.

Author contributions

Conceptualization: M.E.M., J.H.B., S.G.; Methodology: M.E.M., A.V., H.S., J.H.B., S.G.; Formal analysis: M.E.M., H.S.; Investigation: M.E.M., AV., H.S.; Resources: A.V., J.H.B., S.G.; Writing - original draft: M.E.M., S.G.; Writing - review & editing: M.E.M., A.V., H.S., J.H.B., S.G.; Supervision: J.H.B., S.G.; Funding acquisition: S.G.

Funding

This work was supported by Canadian Institutes of Health Research (FDN-143202). M.E.M. was the recipient of a Heart and Stroke Foundation of Canada (HSFC) Pfizer Research Fellowship.

Supplementary information

Supplementary information available online at
https://jcs.biologists.org/lookup/doi/10.1242/jcs.252411.supplemental

Peer review history

The peer review history is available online at
https://journals.biologists.com/jcs/article-lookup/134/7/jcs252411/

References

Abella, J. V., Parachoniak, C. A., Sangwan, V. and Park, M. (2010). Dorsal ruffle microdomains potentiate Met receptor tyrosine kinase signaling and down-regulation. *J. Biol. Chem.* **285**, 24956-24967. doi:10.1074/jbc.M110.127985

Araki, N., Johnson, M. T. and Swanson, J. A. (1996). A role for phosphoinositide 3-kinase in the completion of macropinocytosis and phagocytosis by macrophages. *J. Cell Biol.* **135**, 1249-1260. doi:10.1083/jcb.135.5.1249

Araki, N., Hamasaki, M., Egami, Y. and Hatae, T. (2006). Effect of 3-methyladenine on the fusion process of macropinosomes in EGF-stimulated A431 Cells. *Cell Struct. Funct.* **31**, 145-157. doi:10.1247/csf.06029

Araki, N., Egami, Y., Watanabe, Y. and Hatae, T. (2007). Phosphoinositide metabolism during membrane ruffling and macropinosome formation in EGF-stimulated A431 cells. *Exp. Cell Res.* **313**, 1496-1507. doi:10.1016/j.yexcr.2007.02.012

Bajno, L., Peng, X. R., Schreiber, A. D., Moore, H. P., Trimble, W. S. and Grinstein, S. (2000). Focal exocytosis of VAMP3-containing vesicles at sites of phagosome formation. *J. Cell Biol.* **149**, 697-706. doi:10.1083/jcb.149.3.697

Barbieri, M. A., Kohn, A. D., Roth, R. A. and Stahl, P. D. (1998). Protein kinase B/akt and rab5 mediate Ras activation of endocytosis. *J. Biol. Chem.* **273**, 19367-19370. doi:10.1074/jbc.273.31.19367

Bar-Sagi, D. and Feramisco, J. R. (1986). Induction of membrane ruffling and fluid-phase pinocytosis in quiescent fibroblasts by ras proteins. *Science* **233**, 1061-1068. doi:10.1126/science.3090687

Bloomfield, G. and Kay, R. R. (2016). Uses and abuses of macropinocytosis. *J. Cell Sci.* **129**, 2697-2705. doi:10.1242/jcs.176149

Bohdanowicz, M., Balkin, D. M., De Camilli, P. and Grinstein, S. (2011). Recruitment of OCRL and Inpp5B to phagosomes by Rab5 and APPL1 depletes phosphoinositides and attenuates Akt signaling. *Mol. Biol. Cell* **23**, 176-187. doi:10.1091/mbc.e11-06-0489

Bohdanowicz, M., Schlam, D., Hermansson, M., Rizzuti, D., Fairn, G. D., Ueyama, T., Somerharju, P., Du, G. and Grinstein, S. (2013). Phosphatidic acid is required for the constitutive ruffling and macropinocytosis of phagocytes. *Mol. Biol. Cell* **24**, 1700-12-S1-7. doi:10.1091/mbc.e12-11-0789

Braun, V., Fraisier, V., Raposo, G., Hurbain, I., Sibarita, J.-B., Chavrier, P., Galli, T. and Niedergang, F. (2004). TI-VAMP/VAMP7 is required for optimal phagocytosis of opsonised particles in macrophages. *EMBO J.* **23**, 4166-4176. doi:10.1038/sj.emboj.7600427

Bucci, C., Parton, R. G., Mather, I. H., Stunnenberg, H., Simons, K., Hoflack, B. and Zerial, M. (1992). The small GTPase rab5 functions as a regulatory factor in the early endocytic pathway. *Cell* **70**, 715-728. doi:10.1016/0092-8674(92)90306-W

Buckley, C. M. and King, J. S. (2017). Drinking problems: mechanisms of macropinosome formation and maturation. *FEBS J.* **284**, 3778-3790. doi:10.1111/febs.14115

Chavrier, P., Parton, R. G., Hauri, H. P., Simons, K. and Zerial, M. (1990). Localization of low molecular weight GTP binding proteins to exocytic and endocytic compartments. *Cell* **62**, 317-329. doi:10.1016/0092-8674(90)90369-P

Chen, P.-I., Kong, C., Su, X. and Stahl, P. D. (2009). Rab5 isoforms differentially regulate the trafficking and degradation of epidermal growth factor receptors. *J. Biol. Chem.* **284**, 30328-30338. doi:10.1074/jbc.M109.034546

Cheng, M., Huang, K., Zhou, J., Yan, D., Tang, Y.-L., Zhao, T. C., Miller, R. J., Kishore, R., Losordo, D. W. and Qin, G. (2015). A critical role of Src family kinase in SDF-1/CXCR4-mediated bone-marrow progenitor cell recruitment to the ischemic heart. *J. Mol. Cell. Cardiol.* **81**, 49-53. doi:10.1016/j.yjmcc.2015.01.024

Coppolino, M. G., Kong, C., Mohtashami, M., Schreiber, A. D., Brumell, J. H., Finlay, B. B., Grinstein, S. and Trimble, W. S. (2001). Requirement for N-ethylmaleimide-sensitive factor activity at different stages of bacterial invasion and phagocytosis. *J. Biol. Chem.* **276**, 4772-4780. doi:10.1074/jbc.M007792200

Coppolino, M. G., Dierckman, R., Loijens, J., Collins, R. F., Pouladi, M., Jongstra-Bilen, J., Schreiber, A. D., Trimble, W. S., Anderson, R. and Grinstein, S. (2002). Inhibition of phosphatidylinositol-4-phosphate 5-kinase Ialpha impairs localized actin remodeling and suppresses phagocytosis. *J. Biol. Chem.* **277**, 43849-43857. doi:10.1074/jbc.M209046200

Daste, F., Walrant, A., Holst, M. R., Gadsby, J. R., Mason, J., Lee, J.-E., Brook, D., Mettlen, M., Larsson, E., Lee, S. F. et al. (2017). Control of actin polymerization via the coincidence of phosphoinositides and high membrane curvature. *J. Cell Biol.* **216**, 3745-3765. doi:10.1083/jcb.201704061

Erdmann, K. S., Mao, Y., McCrea, H. J., Zoncu, R., Lee, S., Paradise, S., Modregger, J., Biemesderfer, D., Toomre, D. and De Camilli, P. (2007). A role of the Lowe syndrome protein OCRL in early steps of the endocytic pathway. *Dev. Cell* **13**, 377-390. doi:10.1016/j.devcel.2007.08.004

Fabricant, R. N., De Larco, J. E. and Todaro, G. J. (1977). Nerve growth factor receptors on human melanoma cells in culture. *Proc. Natl. Acad. Sci. USA* **74**, 565-569. doi:10.1073/pnas.74.2.565

Fairn, G. D., Ogata, K., Botelho, R. J., Stahl, P. D., Anderson, R. A., Camilli, P. D., Meyer, T., Wodak, S. and Grinstein, S. (2009). An electrostatic switch displaces phosphatidylinositol phosphate kinases from the membrane during phagocytosis. *J. Cell Biol.* **187**, 701-714. doi:10.1083/jcb.200909025

Feliciano, W. D., Yoshida, S., Straight, S. W. and Swanson, J. A. (2011). Coordination of the Rab5 cycle on macropinosomes. *Traffic Cph. Den.* **12**, 1911-1922. doi:10.1111/j.1600-0854.2011.01280.x

Fujii, M., Kawai, K., Egami, Y. and Araki, N. (2013). Dissecting the roles of Rac1 activation and deactivation in macropinocytosis using microscopic photo-manipulation. *Sci. Rep* **3**, 2385. doi:10.1038/srep02385

Fukuda, M., Kanno, E., Ishibashi, K. and Itoh, T. (2008). Large scale screening for novel rab effectors reveals unexpected broad Rab binding specificity. *Mol. Cell. Proteomics* **7**, 1031-1042. doi:10.1074/mcp.M700569-MCP200

Galperin, E. and Sorkin, A. (2003). Visualization of Rab5 activity in living cells by FRET microscopy and influence of plasma-membrane-targeted Rab5 on clathrin-dependent endocytosis. *J. Cell Sci.* **116**, 4799-4810. doi:10.1242/jcs.00801

Haigler, H. T., McKanna, J. A. and Cohen, S. (1979). Rapid stimulation of pinocytosis in human carcinoma cells A-431 by epidermal growth factor. *J. Cell Biol.* **83**, 82-90. doi:10.1083/jcb.83.1.82

Hasegawa, J., Tokuda, E., Tenno, T., Tsujita, K., Sawai, H., Hiroaki, H., Takenawa, T. and Itoh, T. (2011). SH3YL1 regulates dorsal ruffle formation by a novel phosphoinositide-binding domain. *J. Cell Biol.* **193**, 901-916. doi:10.1083/jcb.201012161

Heo, W. D., Inoue, T., Park, W. S., Kim, M. L., Park, B. O., Wandless, T. J. and Meyer, T. (2006). PI(3,4,5)P3 and PI(4,5)P2 lipids target proteins with polybasic clusters to the plasma membrane. *Science* **314**, 1458-1461. doi:10.1126/science.1134389

Huang, F., Khvorova, A., Marshall, W. and Sorkin, A. (2004). Analysis of clathrin-mediated endocytosis of epidermal growth factor receptor by RNA interference. *J. Biol. Chem.* **279**, 16657-16661. doi:10.1074/jbc.C400046200

Hyvola, N., Diao, A., McKenzie, E., Skippen, A., Cockcroft, S. and Lowe, M. (2006). Membrane targeting and activation of the Lowe syndrome protein OCRL1 by rab GTPases. *EMBO J.* **25**, 3750-3761. doi:10.1038/sj.emboj.7601274

Junemann, A., Filić, V., Winterhoff, M., Nordholz, B., Litschko, C., Schwellenbach, H., Stephan, T., Weber, I. and Faix, J. (2016). A Diaphanous-related formin links Ras signaling directly to actin assembly in macropinocytosis and phagocytosis. *Proc. Natl. Acad. Sci. USA* **113**, E7464-E7473. doi:10.1073/pnas.1611024113

Kay, R. R., Williams, T. D. and Paschke, P. (2018). Amplification of PIP3 signalling by macropinocytic cups. *Biochem. J.* **475**, 643-648. doi:10.1042/BCJ20170785

King, J. S. and Kay, R. R. (2019). The origins and evolution of macropinocytosis. *Philos. Trans. R. Soc. B Biol. Sci.* **374**, 20180158. doi:10.1098/rstb.2018.0158

Lanzetti, L., Palamidessi, A., Areces, L., Scita, G. and Di Fiore, P. P. (2004). Rab5 is a signalling GTPase involved in actin remodelling by receptor tyrosine kinases. *Nat. Cell Biol.* **429**, 309-314. doi:10.1038/nature02542

Lee, W. L., Mason, D., Schreiber, A. D. and Grinstein, S. (2007). Quantitative analysis of membrane remodeling at the phagocytic cup. *Mol. Biol. Cell* **18**, 2883-2892. doi:10.1091/mbc.e06-05-0450

Levin, R., Grinstein, S. and Schlam, D. (2014). Phosphoinositides in phagocytosis and macropinocytosis. *Biochim. Biophys. Acta* **1851**, 805-823. doi:10.1016/j.bbalip.2014.09.005

Li, Q., Lau, A., Morris, T. J., Guo, L., Fordyce, C. B. and Stanley E. F. (2004). A syntaxin 1, Galpha(o), and N-type calcium channel complex at a presynaptic nerve terminal: analysis by quantitative immunocolocalization. *J. Neurosci.* **24**, 4070-4081. doi:10.1523/JNEUROSCI.0346-04.2004

Livak, K. J. and Schmittgen, T. D. (2001). Analysis of relative gene expression data using real-time quantitative PCR and the 2\textminus$\Delta\Delta$CT method. *Methods* **25**, 402-408. doi:10.1006/meth.2001.1262

Loovers, H. M., Kortholt, A., de Groote, H., Whitty, L., Nussbaum, R. L. and van Haastert, P. J. M. (2007). Regulation of phagocytosis in Dictyostelium by the inositol 5-phosphatase OCRL homolog Dd5P4. *Traffic Cph. Den.* **8**, 618-628. doi:10.1111/j.1600-0854.2007.00546.x

Maekawa, M., Terasaka, S., Mochizuki, Y., Kawai, K., Ikeda, Y., Araki, N., Skolnik, E. Y., Taguchi, T. and Arai, H. (2014). Sequential breakdown of 3-phosphorylated phosphoinositides is essential for the completion of macropinocytosis. *Proc. Natl. Acad. Sci. USA* **111**, E978-E987. doi:10.1073/pnas.1311029111

Mao, Y., Balkin, D. M., Zoncu, R., Erdmann, K. S., Tomasini, L., Hu, F., Jin, M. M., Hodsdon, M. E. and Camilli, P. D. (2009). A PH domain within OCRL bridges clathrin-mediated membrane trafficking to phosphoinositide metabolism. *EMBO J.* **28**, 1831-1842. doi:10.1038/emboj.2009.155

Marques, P. E., Grinstein, S. and Freeman, S. A. (2017). SnapShot: Macropinocytosis. *Cell* **169**, 766-766.e1. doi:10.1016/j.cell.2017.04.031

Mellström, K., Heldin, C.-H. and Westermark, B. (1988). Induction of circular membrane ruffling on human fibroblasts by platelet-derived growth factor. *Exp. Cell Res.* **177**, 347-359. doi:10.1016/0014-4827(88)90468-5

Mercer, J. and Helenius, A. (2012). Gulping rather than sipping: macropinocytosis as a way of virus entry. *Curr. Opin. Microbiol.* **15**, 490-499. doi:10.1016/j.mib.2012.05.016

O'Donnell, J. S., Massi, D., Teng, M. W. L. and Mandala, M. (2018). PI3K-AKT-mTOR inhibition in cancer immunotherapy, redux. *Semin. Cancer Biol.* **48**, 91-103. doi:10.1016/j.semcancer.2017.04.015

Porat-Shliom, N., Kloog, Y. and Donaldson, J. G. (2008). A unique platform for H-Ras signaling involving clathrin-independent endocytosis. *Mol. Biol. Cell* **19**, 765-775. doi:10.1091/mbc.e07-08-0841

Racoosin, E. L. and Swanson, J. A. (1989). Macrophage colony-stimulating factor (rM-CSF) stimulates pinocytosis in bone marrow-derived macrophages. *J. Exp. Med.* **170**, 1635-1648. doi:10.1084/jem.170.5.1635

Racoosin, E. L. and Swanson, J. A. (1992). M-CSF-induced macropinocytosis increases solute endocytosis but not receptor-mediated endocytosis in mouse macrophages. *J. Cell Sci.* **102**, 867-880.

Raucher, D., Stauffer, T., Chen, W., Shen, K., Guo, S., York, J. D., Sheetz, M. P. and Meyer, T. (2000). Phosphatidylinositol 4,5-bisphosphate functions as a second messenger that regulates cytoskeleton-plasma membrane adhesion. *Cell* **100**, 221-228. doi:10.1016/S0092-8674(00)81560-3

Rivera, V. M., Wang, X., Wardwell, S., Courage, N. L., Volchuk, A., Keenan, T., Holt, D. A., Gilman, M., Orci, L., Cerasoli, F. et al. (2000). Regulation of protein secretion through controlled aggregation in the endoplasmic reticulum. *Science* **287**, 826-830. doi:10.1126/science.287.5454.826

Roberts, R. L., Barbieri, M. A., Ullrich, J. and Stahl, P. D. (2000). Dynamics of rab5 activation in endocytosis and phagocytosis. *J. Leukoc. Biol.* **68**, 627-632.

Schindelin, J., Arganda-Carreras, I., Frise, E., Kaynig, V., Longair, M., Pietzsch, T., Preibisch, S., Rueden, C., Saalfeld, S., Schmid, B. et al. (2012). Fiji: an open-source platform for biological-image analysis. *Nat. Methods* **9**, 676-682. doi:10.1038/nmeth.2019

Shin, H.-W., Hayashi, M., Christoforidis, S., Lacas-Gervais, S., Hoepfner, S., Wenk, M. R., Modregger, J., Uttenweiler-Joseph, S., Wilm, M., Nystuen, A. et al. (2005). An enzymatic cascade of Rab5 effectors regulates phosphoinositide turnover in the endocytic pathway. *J. Cell Biol.* **170**, 607-618. doi:10.1083/jcb.200505128

Simonsen, A., Lippe, R., Christoforidis, S., Gaullier, J.-M., Brech, A., Callaghan, J., Toh, B.-H., Murphy, C., Zerial, M. and Stenmark, H. (1998). EEA1 links PI(3)K function to Rab5 regulation of endosome fusion. *Nature* **394**, 494-498. doi:10.1038/28879

Spaargaren, M. and Bos, J. L. (1999). Rab5 induces Rac-independent lamellipodia formation and cell migration. *Mol. Biol. Cell* **10**, 3239-3250. doi:10.1091/mbc.10.10.3239

Stauffer, T. P., Ahn, S. and Meyer, T. (1998). Receptor-induced transient reduction in plasma membrane PtdIns(4,5)P2 concentration monitored in living cells. *Curr. Biol.* **8**, 343-346. doi:10.1016/S0960-9822(98)70135-6

Stolz, L. E., Kuo, W. J., Longchamps, J., Sekhon, M. K. and York, J. D. (1998). INP51, a yeast inositol polyphosphate 5-phosphatase required for phosphatidylinositol 4,5-bisphosphate homeostasis and whose absence confers a cold-resistant phenotype. *J. Biol. Chem.* **273**, 11852-11861. doi:10.1074/jbc.273.19.11852

Suh, B.-C., Inoue, T., Meyer, T. and Hille, B. (2006). Rapid chemically induced changes of PtdIns(4,5)P2 Gate KCNQ Ion channels. *Science* **314**, 1454-1457. doi:10.1126/science.1131163

Swan, L. E., Tomasini, L., Pirruccello, M., Lunardi, J. and De Camilli, P. (2010). Two closely related endocytic proteins that share a common OCRL-binding motif with APPL1. *Proc. Natl. Acad. Sci. USA* **107**, 3511-3516. doi:10.1073/pnas.0914658107

Swanson, J. A. (2008). Shaping cups into phagosomes and macropinosomes. *Nat. Rev. Mol. Cell Biol.* **9**, 639-649. doi:10.1038/nrm2447

Veltman, D. M., Williams, T. D., Bloomfield, G., Chen, B.-C., Betzig, E., Insall, R. H. and Kay, R. R. (2016). A plasma membrane template for macropinocytic cups. *eLife* **5**, 12399. doi:10.7554/eLife.20085

Wall, A. A., Condon, N. D., Luo, L. and Stow, J. L. (2018). Rab8a localisation and activation by Toll-like receptors on macrophage macropinosomes. *Philos. Trans. R. Soc. B Biol. Sci.* **374**, 20180151. doi:10.1098/rstb.2018.0151

Wang, J., Guan, E., Roderiquez, G., Calvert, V., Alvarez, R. and Norcross, M. A. (2001). Role of tyrosine phosphorylation in ligand-independent sequestration of CXCR4 in human primary monocytes-macrophages. *J. Biol. Chem.* **276**, 49236-49243. doi:10.1074/jbc.M108523200

Welliver, T. P. and Swanson, J. A. (2012). A growth factor signaling cascade confined to circular ruffles in macrophages. *Biol. Open* **1**, 754-760. doi:10.1242/bio.20121784

Welliver, T. P., Chang, S. L., Linderman, J. J. and Swanson, J. A. (2011). Ruffles limit diffusion in the plasma membrane during macropinosome formation. *J. Cell Sci.* **124**, 4106-4114. doi:10.1242/jcs.091538

Williams, C., Choudhury, R., McKenzie, E. and Lowe, M. (2007). Targeting of the type II inositol polyphosphate 5-phosphatase INPP5B to the early secretory pathway. *J. Cell Sci.* **120**, 3941-3951. doi:10.1242/jcs.014423

Yoshida, S., Hoppe, A. D., Araki, N. and Swanson, J. A. (2009). Sequential signaling in plasma-membrane domains during macropinosome formation in macrophages. *J. Cell Sci.* **122**, 3250-3261. doi:10.1242/jcs.053207

Yoshida, S., Gaeta, I., Pacitto, R., Krienke, L., Alge, O., Gregorka, B. and Swanson, J. A. (2015). Differential signaling during macropinocytosis in response to M-CSF and PMA in macrophages. *Front. Physiol.* **6**, 8. doi:10.3389/fphys.2015.00008

Zerial, M. and McBride, H. (2001). Rab proteins as membrane organizers. *Nat. Rev. Mol. Cell Biol.* **2**, 107-117. doi:10.1038/35052055

Zhu, G., Chen, J., Liu, J., Brunzelle, J. S., Huang, B., Wakeham, N., Terzyan, S., Li, X., Rao, Z., Li, G. et al. (2007). Structure of the APPL1 BAR-PH domain and characterization of its interaction with Rab5. *EMBO J.* **26**, 3484-3493. doi:10.1038/sj.emboj.7601771

Zoncu, R., Perera, R. M., Balkin, D. M., Pirruccello, M., Toomre, D. and De Camilli, P. (2009). A phosphoinositide switch controls the maturation and signaling properties of APPL endosomes. *Cell* **136**, 1110-1121. doi:10.1016/j.cell.2009.01.032